



HAL
open science

Solution self-assembly of fluorinated polymers, an overview

Marc Guerre, Gérald Lopez, Bruno Ameduri, M. Semsarilar, Vincent Ladmiral

► **To cite this version:**

Marc Guerre, Gérald Lopez, Bruno Ameduri, M. Semsarilar, Vincent Ladmiral. Solution self-assembly of fluorinated polymers, an overview. *Polymer Chemistry*, 2021, 12 (27), pp.3852-3877. 10.1039/D1PY00221J . hal-03377919v2

HAL Id: hal-03377919

<https://hal.science/hal-03377919v2>

Submitted on 14 Oct 2021

HAL is a multi-disciplinary open access archive for the deposit and dissemination of scientific research documents, whether they are published or not. The documents may come from teaching and research institutions in France or abroad, or from public or private research centers.

L'archive ouverte pluridisciplinaire **HAL**, est destinée au dépôt et à la diffusion de documents scientifiques de niveau recherche, publiés ou non, émanant des établissements d'enseignement et de recherche français ou étrangers, des laboratoires publics ou privés.

Solution self-assembly of fluorinated polymers, an overview

Marc Guerre, Gérald Lopez, Bruno Ameduri, M. Semsarilar, Vincent Ladmiral

► **To cite this version:**

Marc Guerre, Gérald Lopez, Bruno Ameduri, M. Semsarilar, Vincent Ladmiral. Solution self-assembly of fluorinated polymers, an overview. *Polymer Chemistry*, Royal Society of Chemistry - RSC, 2021, 12 (27), pp.3852-3877. 10.1039/D1PY00221J . hal-03377919

HAL Id: hal-03377919

<https://hal.archives-ouvertes.fr/hal-03377919>

Submitted on 14 Oct 2021

HAL is a multi-disciplinary open access archive for the deposit and dissemination of scientific research documents, whether they are published or not. The documents may come from teaching and research institutions in France or abroad, or from public or private research centers.

L'archive ouverte pluridisciplinaire **HAL**, est destinée au dépôt et à la diffusion de documents scientifiques de niveau recherche, publiés ou non, émanant des établissements d'enseignement et de recherche français ou étrangers, des laboratoires publics ou privés.

REVIEW

Solution self-assembly of fluorinated polymers, an overview

Cite this: DOI: 10.1039/d1py00221j

Q1

Marc Guerre, *^a Gérald Lopez, ^b Bruno Améduri, ^b Mona Semsarilar ^c and Vincent Ladmiral *^b

Fluoropolymers constitute an attractive family of polymeric materials with remarkable properties such as high resistance to chemicals, UV and heat, ferroelectricity and piezoelectricity for semi-crystalline polymers, to name a few. The incorporation of fluorinated moieties in a polymer can confer unique properties. Due to the fluorine atom's high electronegativity and the peculiar interactions of the fluorinated group, such polymers readily self-assemble in solution and often lead to original morphologies endowed with rare properties. Thanks to advances made in organic and polymer chemistry, a large variety of fluorinated monomers and polymers have been used to design fluorinated copolymer architectures. This review gives an overview of the current state of the art of the solution self-assembly of these fluorinated copolymer architectures.

Received 18th February 2021.
Accepted 23rd May 2021

DOI: 10.1039/d1py00221j

rs.c.li/polymers

1. Introduction

Recent years have witnessed a continuous increase of interest in the development of nanoscale technologies dedicated to the production and control of the self-assembly of nano-objects

into organized patterns.^{1–5} The self-assembly of block copolymers was particularly investigated through solution-based processes, which, under particular conditions, can form sophisticated morphologies,^{6–9} such as spheres, cylinders, bilayer sheets and vesicles (polymersomes), to name a few. The morphologies of the self-assembled structures depend mainly on the molecular and structural characteristics of the polymer building blocks, such as composition, number of segments, segment lengths, block sequence, interactions between blocks, interactions of the blocks with the solvent, and architecture.^{10,11} The self-assembled morphologies are also substantially affected by the solution self-assembly conditions

^aLaboratoire des IMRCP, Université de Toulouse, CNRS UMR 5623, Université Paul Sabatier, 118 route de Narbonne, 31062 Toulouse Cedex 9, France.

E-mail: marc.guerre@univ-tlse3.fr

^bICGM, Univ Montpellier-CNRS-ENSCM, Montpellier, France.

E-mail: vincent.ladmiral@enscm.fr

^cIEM, Univ Montpellier-CNRS-ENSCM, Montpellier, France



Marc Guerre

Marc Guerre completed his Ph.D. degree in polymer chemistry in 2017 from the Chemistry School of Montpellier (ENSCM, France) where he studied and developed RAFT polymerization techniques applied to fluoropolymers. Then, he joined Prof. Filip Du Prez's laboratory at Ghent University to work on the development of fluorinated vitrimers. Since October 2019, he has been a CNRS researcher at the IMRCP laboratory (Toulouse, France) in

the team Precision Polymers by Radical Process (P₃R). His research interest includes the synthesis of well-defined polymeric systems directed towards self-assembled structures for the design of sophisticated dynamic covalent materials.



Gérald Lopez

Gérald Lopez is an R&T Engineer at the SAFRAN Group's Materials and Processes Department. He began his studies at the University of Montpellier, then worked on the chemistry of carbohydrates, gaining his Ph.D. in 2006 at the University of Rennes. He held several postdoctoral positions in the field of bio-organic chemistry in France (Pasteur Institute) and in New Zealand (The University of Canterbury). Then, he spent 8

years at the Charles Gerhard Institute in Montpellier working on fluoropolymers as a research engineer. He is currently in charge of polymers for aerospace electrical and electronic applications at the Paris-Saclay SAFRAN facility.

(assembly methods, solvent mixtures), external stimuli (e.g. pH, ionic strength, temperature, light irradiation, etc.), or other polymer characteristics (such as crystallinity, donor-acceptor interactions, H-bonds, etc.).¹²⁻¹⁵ However, the resulting assemblies are often kinetically trapped because of the inability of the system to reach thermodynamic equilibrium. This implies that one polymer can potentially produce various (meta)stable morphologies of various topological complexities depending on the path taken toward self-assembly.^{16,17} The introduction of fluorinated segments into block copolymers endows the final self-assembled morphologies with additional properties and often significantly modifies the self-assembly process due to the peculiar behaviour of fluorinated groups.¹⁸ This exotic family of copolymers possesses original self-assembly behaviour due to their incompatibility with nonfluorinated segments, which promotes a strong phase segregation.¹⁹ As a result, the behaviour of amphiphilic fluorinated block copolymers remains difficult to explain due to the tendency of the fluorine-rich segments to segregate from both the hydrophilic and lipophilic segments, which then result in a plethora of possible morphologies.^{10,20,21} In addition, the description of these self-assembly behaviours is still largely phenomenological.

This review presents a comprehensive overview of the advances made in the self-assembly of fluorinated block copolymers. In the first section, the common self-assembly methods are briefly described and help the reader to understand how the morphologies described in the remainder of the review were obtained. This methods section is then followed by 6 sections dedicated to different classes of fluorinated monomers and polymers ((meth)acrylates, styrenic, etc.). These sections present and discuss the most relevant articles published to date. Special attention has been paid to multicompartment micelles, stimuli responsive nano-objects and polymerisation-induced self-assembly because of particular inter-

est from the community for these objects and/or polymerisation techniques as well as the promising applications they could offer.

1.1. Self-assembly methods

Method 1: The block copolymer is gradually added in a specific solvent to one of the blocks under vigorous stirring.

Method 2: The block copolymer is dissolved in a good solvent then added to a selective solvent for one of the blocks of the polymer under vigorous stirring.

Method 3: Addition of a block copolymer solution in a good solvent to a selective solvent and removal of the good solvent by evaporation (under vacuum or not).

Method 4: Addition of a block copolymer solution in a good solvent to a selective solvent and removal of the good solvent by dialysis.

Method 5: Addition of a selective solvent to a block copolymer solution in a good solvent and removal of the good solvent by evaporation or distillation.

Method 6: Addition of a selective solvent to a block copolymer solution in a good solvent and removal of the good solvent by dialysis.

Method 7: Dialysis of a solution of the block copolymer in a good solvent against a selective solvent.

2. Poly(fluorinated(meth)acrylate)-based copolymers

2.1. Conventional self-assembly

Poly(fluorinated (meth)acrylate) copolymers possess unique properties, such as low surface energies, low friction coefficients, and high insolubility in conventional solvents.^{22,23} Thanks to the advent of reversible-deactivation radical polymerisation (RDRP) techniques, a large number of well-defined



Bruno Améduri

Bruno Améduri is CNRS Senior Researcher and his main interests focus on the synthesis and characterization of fluorinated monomers, telomers, and copolymers for applications such as surfactants, elastomers, coatings, fuel cell membranes, polymer electrolytes for Li-ions batteries, and electroactive films. Coauthor of 5 books, 50 reviews or book chapters, 390 publications and co-inventor of 80 patents, he is also a member of the American

and French Chemical Societies and on the Editorial Boards of J. Fluorine Chemistry, Eur. Polym. J. and Polym. Bull. Still playing football, he is an active member of the "Rire" association and visits sick children in hospitals.



Mona Semsarilar

Mona Semsarilar earned her Ph.D. from the University of Sydney in 2010 under the supervision of Prof. S. Perrier. She then moved to the University of Sheffield (UK) to work on polymerization induced self-assembly (PISA) under the supervision of Prof. S. Armes (FRS). In 2015 she was recruited by the French National Research Organization (CNRS) as a research scientist based in the European Institute of Membranes (IEM) in Montpellier (France). In 2019, she received her habilitation from the University of Montpellier. Her research focuses on using synthetic chemistry to tailor molecular design and control self-assembly to prepare porous materials for membrane applications.

1 block copolymers (BCPs) based on fluorinated (meth)acrylates
 5 have been synthesised. However, the self-assemblies of poly
 (fluorinated (meth)acrylate)-based BCPs have been relatively
 understudied compared with their fully hydrogenated counter-
 parts. At the beginning of the century, fluorinated block copo-
 10 polymers and especially triphilic copolymers (amphiphilic copo-
 lymeric composed of a hydrophilic segment and two hydro-
 phobic yet mutually incompatible segments, thus generating
 local microphase separation) attracted much interest. These
 BCPs possess the exceptional ability to form multicompart-
 15 ment micelles with hydrophobic, fluorophilic and hydrophilic
 separated domains.²¹ These unusual morphologies, which
 favour the independent take up and release of different (and
 potentially incompatible) compounds, are thought to be prom-
 ising for drug delivery and controlled release strategies.^{24–26}

This section dealing with the self-assembly of fluorinated
 (meth)acrylate-based block and hyperbranched copolymers is
 classified by families of fluorinated (meth)acrylates with an
 increasing number of fluorine atoms (Scheme 1). One should
 20 bear in mind that poly(fluorinated (meth)acrylates) can be
 amorphous or crystalline depending on the length of their
 fluoroalkyl side chains. This characteristic can impact on the
 structure of the self-assemblies (*e.g.* polyfluoroalkyl acrylates
 bearing perfluorinated side chains longer than 6 carbons are
 25 usually liquid crystalline (LC) and very hydrophobic). The use
 of the LC properties of fluorinated copolymers is specifically
 addressed in the sections dealing with side chains bearing at
 least C₈F₁₇ units due to their outstanding ability to form rigid
 and well-defined cylindrical micelles *via* crystallization-driven
 self-assembly (CDSA).

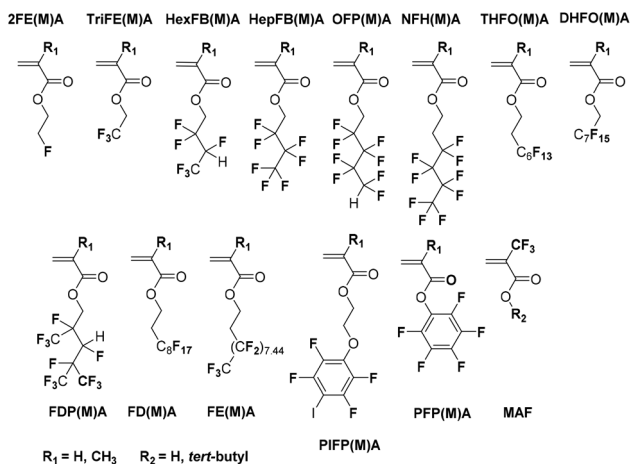
2.1.1. 2-Fluoroethyl (meth)acrylate (2FE(M)A). In 2011, He
 30 *et al.* reported the self-assembly of linear triblock terpolymers
 consisting of P*n*BMA-*b*-PMMA-*b*-P2FE(M)A (P*n*BMA = poly(*n*-
 butyl methacrylate) and PMMA = poly(methyl methacrylate))
 synthesised by sequential RAFT (reversible addition–fragmen-
 tation chain transfer) polymerisation.²⁷ The copolymers were
 self-assembled using method 2 in a mixture of THF (good



Vincent Ladmiral

Vincent Ladmiral graduated
 from the National Graduate
 School of Chemistry of
 Montpellier in 1998, and
 received his Ph.D. from the
 University of Warwick in 2006.
 After postdoctoral fellowships at
 the University of Kyoto, the
 University of Sydney, the
 University of New South Wales
 and the University of Sheffield,
 he was appointed CNRS
 Research Fellow in 2012 at the
 Institut Charles Gerhardt of

Montpellier. His research interests focus on the structure–property
 relationships of polymers and materials.



Scheme 1 Structures of the referred to self-assembled fluorinated
 (meth)acrylate copolymers. 2-Fluoroethyl (meth)acrylate (2FE(M)A),
 2,2,2-trifluoroethyl (meth)acrylate (TriFE(M)A), 2,2,3,4,4,4-hexafluorobu-
 tyl (meth)acrylate (HexFB(M)A), 2,2,3,3,4,4,4-heptafluorobutyl (meth)
 20 acrylate (HepFB(M)A), 2,2,3,3,4,4,5,5-octafluoropentyl (meth)acrylate
 (OFP(M)A), 3,3,4,4,5,5,6,6,6-nonafluorohexyl methacrylate (NFHMA),
 1*H*,1*H*,2*H*,2*H*-perfluorooctyl methacrylate (THFOMA), 1*H*,1*H*-perfluoro-
 octyl methacrylate (DHFOMA), dodecafluoroheptyl methacrylate
 (FDPMA), 1*H*,1*H*,2*H*,2*H*-perfluorodecyl (meth)acrylate (FD(M)A), perfluoro-
 alkyl ethyl methacrylate (FEMA), iodotetrafluorophenoxy methacry-
 late (IFPMA), pentafluorophenyl methacrylates (PFP(M)A), 2-(trifluoro-
 methyl)acrylic acid (MAF) and its ester.

solvent) and methanol (bad solvent) and led to well-defined
 30 and uniform spherical aggregates. The lack of other articles
 dealing with the self-assembly of 2FE(M)A-containing BCP
 likely lies in the minor influence of the fluorinated atom over
 the final morphologies.

2.1.2. 2,2,2-Trifluoroethyl (meth)acrylate (TriFE(M)A)

Block copolymers. In 2012, Whittaker's group reported the
 effect of the solvent on the self-assembly behaviour of PAA-*b*-P
 (*n*BA-*co*-TriFEA) (AA = acrylic acid, *n*BA = *n*-butyl acrylate) copo-
 35 lymeric prepared by sequential atom transfer radical polymerisa-
 tion (ATRP).²⁸ The triblock copolymers were initially dissolved
 in acetone or DMF and analysed by transmission electron
 microscopy (TEM). At that point, the copolymer solutions were
 dialyzed against deionized water and characterized by TEM. In
 40 pure DMF, large aggregates were observed, while, in acetone,
 cylindrical structures were formed, consistent with predictions
 based on relevant polymer–solvent interaction parameters. Upon
 addition of water, both systems formed cylindrical micelles. The
 same group also reported multifunctional hyperbranched copoly-
 45 mers containing iodine and fluorine atoms for applications as
 magnetic resonance imaging (MRI) contrast agents and bimodal
 imaging agents.²⁹

Later, in 2014 Li *et al.* reported the self-assembly of PMMA-
b-PTriFEA diblock copolymer synthesised by RAFT poly-
 50 merisation. The self-assembled morphologies were relatively
 ill-defined with the formation of large aggregates (>μm) due to
 the use of water as the structuring solvent (bad solvent for
 both blocks).³⁰ The same year, Muraro *et al.* reported the syn-

thesis of P_{OE}GMA-*b*-P_{Tri}FEMA (OEGMA = oligoethylene glycol methacrylate) block copolymers by RAFT.³¹ These copolymers formed well-defined sub-100 nm spherical particles using methods 1 and 6. With a view to develop stimuli-responsive aggregates, Zhang and Zhu prepared CO₂- and O₂-responsive polymer vesicles consisting of a hydrophilic polyethylene glycol (PEG) block, a CO₂-responsive PDEAEMA (poly(2-diethylamino)ethylmethacrylate) block and an O₂-responsive P_{Tri}FEMA block copolymers.³²

The PEG-*b*-PDEAEMA-*b*-P_{Tri}FEMA triblock copolymer was synthesised by ATRP in 2 steps from PEG macro-CTA (CTA = chain-transfer agent) and self-assembled in water into vesicular nanoaggregates using method 4. When treated with CO₂, the vesicular morphology transformed into objects of smaller size, to accommodate the increased interfacial free energy. When treated with O₂, the vesicular morphology was preserved, but its volume expanded (Fig. 1). This phenomenon was attributed to the intermolecular interaction between O₂ and P_{Tri}FEMA, which slightly increased the water solubility of the fluorinated hydrophobic block.

Q3 *Gradient, graft, hyperbranched copolymers.* In addition to block copolymer architectures, other architectures, such as gradient or graft copolymers, were also studied. Chen *et al.* reported the self-assembly in different solvent mixtures of PAA-*grad*-P_{Tri}FEMA gradient copolymers prepared by RAFT.³³ Although the authors claimed that the copolymers self-assembled in selective solvents to form crew-cut micelles with different ordered structures and a certain degree of tunability depending on the solvent, their conclusions may be surmised considering the TEM images provided. Graft copolymers were reported by Xu *et al.* who studied the self-assembly of bottle-brush polymers composed of P_{Tri}FEMA side chains and polynorbornene backbones, synthesised *via* ATRP and ring opening metathesis polymerisation (ROMP).³⁴ A PNB-*g*-P_{Tri}FEMA graft copolymer was self-assembled using method 1

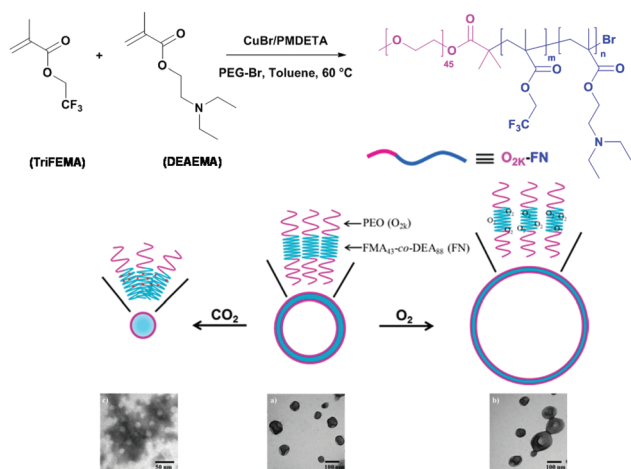


Fig. 1 Synthesis routes to CO₂- and O₂-sensitive block copolymers. Schematic representations and TEM pictures of CO₂- and O₂-driven self-assemblies in water of PEG-*b*-PDEAEMA-*b*-P_{Tri}FEMA triblock copolymers. Adapted with permission from ref. 32. Copyright 2014 ACS.

and formed near-spherical particles with a diameter of *ca.* 10 nm, corresponding to the dimensions of a single chain. When the *L/D* ratio was gradually increased (with *L* standing for the backbone length and *D* the side chain length), the self-assembled microstructures evolved nicely and transitioned from elongated shapes toward “spherical” particles with a diameter of *ca.* 25 nm, suggesting partial coiling of the backbone. Wooley and coworkers³⁵ synthesised hyperbranched-star amphiphilic TriFEMA-based fluorinated polymers with a core-shell morphology. These amphiphilic fluorinated hyperbranched-star polymers were then self-assembled into 20 nm polymer micelles, which presented attractive properties for applications in ¹⁹F MRI.

2.1.3. 2,2,3,4,4,4-Hexafluorobutyl (meth)acrylate (HexFB(M)A) Block copolymers. Diblock copolymers³⁶ containing HexFBMA have been much less studied compared with triblock copolymers. In 2014, Feng and co-workers³⁷ pioneered the synthesis and self-assembly of CO₂-switchable multi-compartment micelles (MCMs) prepared from a linear ABC triblock copolymer synthesised by RAFT polymerisation. The ABC block copolymer was composed of a PHexFBMA block, a hydrophilic polyethylene oxide (PEO) block, and a CO₂-responsive block of PDEAEMA. The triblock copolymer was self-assembled using method 7. In the first place, the micelles appeared as spheres with only a little phase segregation in the core (Fig. 2a). However, after treatment with CO₂, the aggregates showed clearly segregated microdomains typical of MCMs with various phase-segregated morphologies, such as “hamburgers” (1, Fig. 2b), “reverse hamburgers” (2, Fig. 2b),

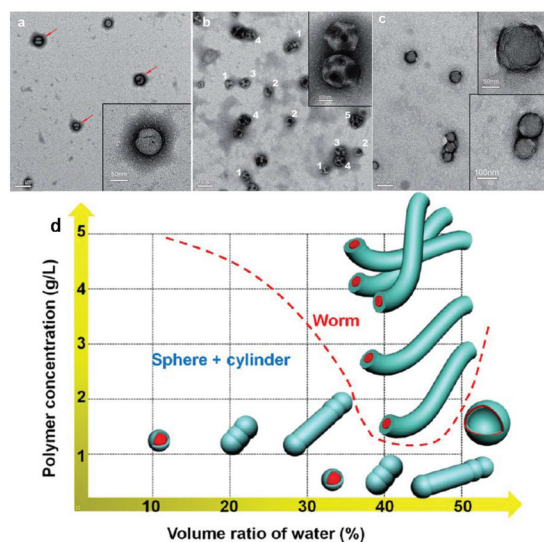


Fig. 2 (a–c) TEM images of PEG-*b*-PHexFBMA-*b*-PDEAEMA triblock copolymer self-assemblies in water. (a) Before CO₂ bubbling, (b) after CO₂ bubbling, and (c) after CO₂ removal by N₂ bubbling. Reproduced with permission from ref. 37. Copyright 2014 RSC. (d) Phase diagram of the PEG-*b*-PHexFBMA-*b*-PDEAEMA triblock copolymer in water/ethanol mixed solvent as a function of volume ratio of water and polymer concentration. Reproduced with permission from ref. 38. Copyright 2015 ACS.

“clovers” (3, Fig. 2b), “soccer ball” (4, Fig. 2b) and more complicated structures (5, Fig. 2b). Interestingly, these morphological transitions were completely reversible and could be switched “on” and “off” by treatment with CO₂ and N₂ *via* simple protonation and deprotonation of the tertiary amine groups.

When these authors employed self-assembly method 1, worm-like micelles (WLMs) were formed.³⁸ Under this regime, an evolution from spherical micelles to short rods, cylinders, and finally worm-like micelles was observed when the water content of a water/ethanol binary mixture was increased from 0 to 50% (Fig. 2d). The authors also showed that higher polymer concentrations favoured the formation of WLMs, while the morphology was less affected by the length of the PDEAEMA block. The latest study of the same group reported the synthesis of a series of PEG-*b*-PHexFBMA-*b*-PDEAEMA triblock copolymer nanoparticles. The majority of morphologies obtained were spherical particles even after exposure to CO₂. Only triblock copolymers with volume fractions of 0.34 to 0.38 of PHexFBMA transformed from spherical micelles to multi-compartment micelles after reaction with CO₂.³⁹

Graft copolymers. Graft copolymers were the second class of macromolecular architectures predominantly investigated for HexFPMA. Xiong *et al.* described the synthesis, self-assembly and encapsulation properties of a series of amphiphilic graft copolymers (PHexFBMA-*g*-PSPEG) synthesised by conventional free radical polymerisation of a PHexFBMA backbone and PEG side chains (SPEG was synthesised by reacting methoxy poly(ethylene glycol) (MPEG) with *p*-chloromethylstyrene in THF).⁴⁰ Self-assembly using method 1 resulted in the formation of spherical morphologies that evolved into worm- and vesicle-like structures upon the addition of bovine serum albumin. Later, in 2016, Pang's group⁴¹ reported the preparation of well-defined thermoresponsive block-graft copolymer, PHexFBMA-*b*-(PGMA-*g*-PNIPAM) using ATRP and copper-catalyzed azide-alkyne cycloaddition (CuAAC) coupling reaction (PNIPAM = poly(*N*-isopropyl acrylamide) and PGMA = poly(poly(glycidyl methacrylate))). The copolymers were self-assembled using method 5. TEM images showed stable spherical nanoparticles with diameters of 30–40 nm at 20 °C. Larger and more irregular particles were formed at more elevated temperatures (40–60 °C) due to the phase transition of the thermosensitive PNIPAM segments.

2.1.4. 2,2,3,3,4,4,4-Heptafluorobutyl (meth)acrylate (HepFB(M)A). In 2011, Laschewsky's team reported original morphologies from the self-assembly of amphiphilic triblock copolymers composed of hydrophilic poly(oligoethylene glycol acrylate) (POEGA), lipophilic PBzA (poly(benzyl acrylate), and fluorophilic HepFBA, synthesised by sequential RAFT polymerisations.⁴² The self-assembly was performed in water using method 5. The resulting morphologies obtained after annealing were unique with segregated domains forming structures resembling a “soccer ball” (Fig. 3a) or bi-spherical/acorn micelles (Fig. 3b). Studies on different copolymer compositions revealed that the morphologies depended on the length of the individual blocks as well as the block sequence. Quite uniquely, it was

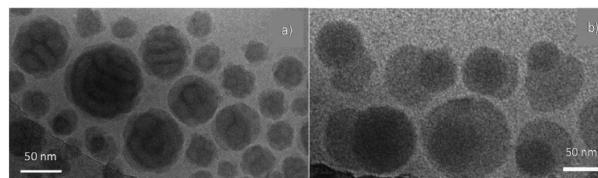


Fig. 3 (a) “Soccer ball” morphologies observed in cryo-TEM images of a 0.5 wt% solution of PBzA₄₅-*b*-POEGA₄₀-*b*-PHepFBA₃₀ in water after annealing for 2 weeks at 75 °C. (b) Bi-spherical morphologies observed in cryo-TEM images of a 0.5 wt% solution of PBzA₄₅-*b*-POEGA₁₇₅-*b*-PHepFBA₄₀ in water after annealing for 2 weeks at 75 °C. Reproduced with permission from ref. 42. Copyright 2011 ACS.

demonstrated that the fluorinated and hydrocarbon low molar mass compounds could be solubilised selectively in the respective fluorophilic and lipophilic domains.

Following this work, Zhou *et al.* reported the synthesis and self-assembly of PS-*b*-PHepFBMA (PS = polystyrene) diblock copolymers synthesised by sequential ATRP.⁴³ The diblock copolymers were self-assembled in THF/EtOAc binary mixture using method 2. The authors showed that the assemblies evolved from spheres to vesicles with an increasing content of EtOAc in the solvent mixture. In 2015, Singha and co-workers reported the RAFT synthesis of PPEGMA-*b*-PHepFBA diblock copolymer and their self-assembly in water using method 1, which resulted in the formation of spherical micelles.⁴⁴ This diblock copolymer was also successfully used as a surfactant and macro-RAFT agent (surf-RAFT agent) for the mini-emulsion polymerisation of styrene. The same authors also reported the synthesis and self-assembly of PMMA-*b*-PHepFBA diblock copolymers,⁴⁵ which self-assembled *via* method 2 in methyl ethyl ketone:tetrahydrofuran (MEK:THF) binary mixtures. The self-assembled morphologies, depending on the THF:MEK volume ratios, were claimed to be micelles, worms and nanotubes, although the evidence provided may not be sufficiently convincing. In a different approach, Luo and co-workers employed (PDMS-*b*-PMMA-*b*-PHepFBMA, a silicone-containing triblock copolymer) to stabilise gold nanoparticles (PDMS = poly(dimethyl siloxane)).⁴⁶ They also reported the self-assembly of amphiphilic gradient copolymer poly(AA-*grad*-HepFBMA) in THF/H₂O mixtures (16 ≤ H₂O (%) ≤ 84), forming mainly ill-defined morphologies, containing a few unusual morphologies, such as cubes or circles.⁴⁷

2.1.5. 2,2,3,3,4,4,5,5-Octafluoropentyl (meth)acrylate (OFP(M)A). The group of Ni was the first to study the self-assembly of POFPPMA-containing copolymers. In 2007, they pioneered the synthesis (*via* oxyanion-initiated polymerisation)⁴⁸ and self-assembly of fluorinated hyperbranched star-block copolymers composed of hyperbranched poly[3-ethyl-3-(hydroxymethyl)oxetane] cores, and PDMAEMA (poly((2-dimethylamino)ethyl methacrylate)) and POFPPMA as the arms.⁴⁹ Using method 1 in acidic aqueous solution, the copolymers self-organized into multicompartiment micelles. When DMF:water binary mixture was used, the copolymer with a short PDMAEMA segment, self-assembled into well-dispersed multi-

1 compartment micelles, while a copolymer with twice as long PDMAEMA formed nanofibers/thread-like morphologies. The same team later worked on more defined block copolymers architectures.⁵⁰ Using the same synthesis procedure, they synthesised POFPMA-*b*-PEO-*b*-PPO-*b*-PEO-*b*-POFPMA (PPO = polypropylene oxide), an amphiphilic pentablock copolymer. Self-assembly using method 1 led to the formation of well-defined frozen micelles, while method 3 resulted in more complex morphologies, such as multicompartment micelles or vesicles, depending on the length of the fluorinated block. They also investigated the self-assembly of double-hydrophilic, fluorinated monomethyl end-capped poly(ethylene glycol)-*b*-poly[2-(dimethylamino)ethyl methacrylate]-*b*-poly(2,2,3,3,4,4,5,5-octafluoropentyl methacrylate) (MePEG-*b*-PDMAEMA-*b*-POFPMA) triblock copolymer, which was synthesised *via* oxyanion-initiated polymerisation.⁵¹ These triblock copolymers were self-assembled using method 1 in water at pH 7. Spherical morphologies were mainly observed, but a transition from sphere to rod morphologies was observed when the lengths of the MePEG and PDMAEMA blocks were reduced. In another report, they elegantly studied and compared the self-assembly behaviour of PIB-*b*-PDMAEMA-*b*-POFPMA (PIB = polyisobutylene) and PS-*b*-PDMAEMA-*b*-POFPMA triblock copolymers using method 1.⁵² This study demonstrated that the flexible PIB block strongly influenced the nature of the self-assembled morphologies, which evolved from spherical multicompartment micelles to fiber-like aggregates, nanotubules, and finally rod-like aggregates upon increasing the polymer concentration (Fig. 4, left). Conversely, the rigid PS-based system self-assembled into multicompartment micelles, hamburger-like structures and flowerlike nanoparticles (Fig. 4, right). Zhuang's group reported, in two complementary studies, the self-assembly behaviour of miktoarm POFPMA-based block copolymers prepared by ATRP and CuAAC coupling.^{53,54} Method 4 was used for self-assembly, which resulted in the formation of spherical particles. Block copolymers with a longer POFPMA block formed an array of nanostructures, ranging from simple and patchy spherical micelles and aggregates to vesicles.

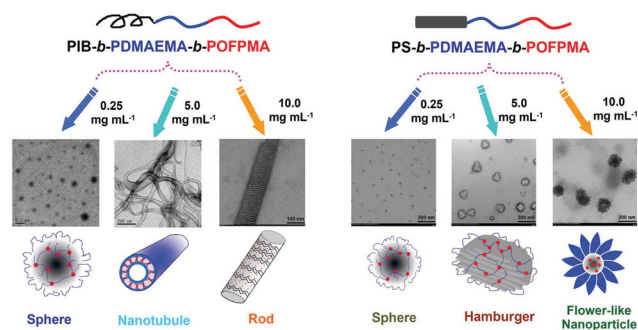


Fig. 4 Schematic illustration and TEM images of numerous hierarchical assemblies formed from PIB-*b*-PDMAEMA-*b*-POFPMA and PS-*b*-PDMAEMA-*b*-POFPMA triblock terpolymers. Reproduced with permission from ref. 52. Copyright 2016 RSC.

Other morphologies were also observed, such as raspberry-like, concave patchy, brush-like, segmented worm-like micelles and perforated stomatocytes. Similar triblock copolymers based on PEG, PLA (poly(lactic acid)) and POFPMA were also reported with potential application as an ultrasound contrast agent.⁵⁵

2.1.6. 3,3,4,4,5,5,6,6,6-Nonafluorohexyl methacrylate (NFHMA). NFHMA-based copolymers and their self-assembly are scarce in the literature. In 2004, Matsuoka's group reported, for the first time, the synthesis and self-assembly of well-defined PNaMA-*b*-PNFHMA (NaMA = sodium methacrylate) amphiphilic diblock copolymers synthesised by anionic polymerisation.⁵⁶ Using method 1, these block copolymers formed micelles in aqueous solution. Dynamic light scattering (DLS), small angle X-ray scattering (SAXS) and small angle neutron scattering (SANS) analyses revealed that these diblock copolymers formed larger micelles than their nonfluorinated analogs. The authors also demonstrated the fluorophilicity of PNaMA-*b*-PNFHMA diblock copolymers by selective solubilisation of fluorinated low molar mass compounds (decafluorobiphenyl and 2,6-dimethylnaphthalene). Later, Wang *et al.* described the aqueous self-assembly (method 3) of MePEG-*b*-PCL-*g*-PNFHMA terpolymers synthesised by ring opening polymerisation (ROP) and ATRP (PCL = poly(ϵ -caprolactone)).⁵⁷ Because of the incompatibility of PCL and PNFHMA, well-segregated Janus cores were formed. These findings demonstrated once again that the architecture of each hydrophobic segment could play a significant role in the formation of specific compartmentalized structures.

2.1.7. 1H,1H,2H,2H-Perfluorooctyl methacrylate (THFOMA). In 2003, Hussain *et al.* described the self-association properties of di- and ABA triblock copolymers synthesised by ATRP, containing PEO as the hydrophilic block (B) and PTHFOMA as the hydrophobic block (B).⁵⁸ The block copolymers were self-assembled in water using method 1 and were analysed by DLS and TEM. DLS revealed the existence of various types of aggregates in solution, including single chains, micelles, and large clusters. Surprisingly, only large clusters were detected in the case of the triblock copolymers. In addition, depending on the initial concentration, single chain micelles, fibrous networks, and ill-defined aggregates were revealed by TEM. Then in 2004, Hwang *et al.* reported the synthesis by ATRP of diblock and statistical copolymers from OEGMA and THFOMA and their self-assembly using method 1 in water and chloroform.⁵⁹ In water, spherical micelles were formed, while, in chloroform, a mixture of worm-like micelles and large aggregates were observed, depending on the blocks lengths. In 2016, Sawamoto reported multipode self-folding copolymers obtained from thermoresponsive intramolecular self-assembly of PEG-methacrylate and THFOMA random copolymers in water, DMF, and 2H,3H-perfluoropentane (2HPFP).⁶⁰ The random copolymers were efficiently prepared by ruthenium-catalysed living radical copolymerisation. They displayed various self-folding structures and local associations. The authors also showed that replacing poly(ethylene glycol) by trehalose caused an increase in the polarity difference with

the fluorinated hydrophobic segment and changed the aggregation state of the polymer in water. The PEG-fluorinated and trehalose/PEG-fluorinated amphiphilic random copolymers were the most efficient at encapsulating novaluron, a fluorinated agrochemical. The presence of the agrochemical exerted a substantial influence on the self-assembly of the polymers, demonstrating that fluorous interactions altered the intramolecular self-folding behaviour and intermolecular polymer association, which led to the formation of well-defined nanoparticles.⁶¹ In addition, they designed A/C-B/C random block copolymers, introducing hydrophobic dodecyl ($-C_{12}H_{25}$, **A**) and hexafluorooctyl pendant groups ($-C_2H_4C_6F_{13}$, **B**) into the blocks, and hydrophilic poly(ethylene glycol) pendant groups (PEG, **C**) randomly placed in both blocks. By controlling the DP and the composition of this block copolymer, self-assembly led to the formation of double core, tadpole and multi-compartment micelles in water.⁶²

2.1.8. 1H,1H-Perfluorooctyl methacrylate (DHFOMA). The synthesis and self-assembly of DHFOMA copolymers have exclusively been reported by Lee *et al.*⁶³ They synthesised block copolymers of hydrophilic PEO and hydrophobic PDHFOMA by ATRP of PDHFOMA from a PEO-macro-initiator. The direct dissolution of the block copolymer in chloroform (method 1) resulted in the formation of well-ordered spherical particles with average diameter of 12–26 nm.

2.1.9. Dodecafluoroheptyl methacrylate (FDPMA). Xu and Liu examined PAA-*b*-PFDPMA diblock copolymers for the first time.⁶⁴ Synthesised by RAFT, these amphiphilic block copolymers were self-assembled using method 6 with 2-butanone as the good solvent and water:methanol binary mixtures as the selective solvent (2-butanone and methanol were removed by dialysis). TEM revealed various morphologies: spheres, rods, and vesicles, depending on the initial water fraction in the water/methanol binary mixtures. The addition of fluorinated hydrophobic homopolymers converted the spheres, rods, and vesicles into large spheres. Dong *et al.* studied the self-assembly of PMMA-*b*-PFDPMA diblock copolymers synthesised by ATRP.⁶⁵ These diblock copolymers were self-assembled using method 1 in chloroform, THF and trifluorotoluene (TFT). In chloroform, comb-shape particles were observed (Fig. 5a). In THF, spherical particles were formed with dark fluorinated centres and lighter hydrogenated edges (Fig. 5b). In TFT, the aggregates were simply constituted of homogeneous unimers

due to the good solubility of both PMMA and PFDPMA in the solvent (Fig. 5c). Multiblock copolymers were also investigated by Tuo *et al.*, who synthesised tetraphenylethane-based polyurethane (PUMI) as a macroiniferter for the conventional radical polymerisation of FDPMA. This polymer self-assembled into various nanostructures during the course of polymerisation.⁶⁶ The incompatibility of FDPMA and PUMI led to a significant decrease in the solubility of PUMI in DMF with the addition of FDPMA monomer, and drove the formation of multicore particles. These morphologies evolved into arrays of disk-like structures, while the smallest particles formed nanofibers.

Pan *et al.* reported the synthesis and self-assembly of linear POSS-PMMA-*b*-PFDPMA (POSS = polyhedral oligomeric silsesquioxane) and star-shaped (s-POSS-PMMA-*b*-PFDPMA) diblock copolymers.⁶⁷ Self-assemblies were achieved in THF using method 1 and led to the formation of core/shell micelles. In another study, the same group synthesised 1/2/4/6-arm architectures of PMMA-*b*-POSS-*b*-PFDPMA. All four structures self-assembled into spherical core-shell micelles (100–250 nm) in THF. The size of the micelles was inversely related to the number of arms (smaller aggregates with an increasing number of arms).⁶⁸

2.1.10. 1H,1H,2H,2H-Perfluorodecyl (meth)acrylate (FD(M)A). FDMA-based copolymers are by far the most studied acrylic-based fluorinated polymers. This is due to their high fluorophilicity that could lead to unusual morphologies, as well as the tendency to form crystalline cylindrical micelles due to the presence of C_8F_{17} side chains and their liquid crystalline property. The first self-assembly of FD(M)A-based copolymers was reported in 2000 by Imae *et al.* who investigated the self-assembly of PMMA-*b*-PFDMA and PtBMA-*b*-PFDMA (*t*BMA = *tert*-butyl methacrylate) diblock copolymers in acetonitrile and chloroform.⁶⁹ Spherical aggregates were observed by cryo-TEM in both solvents. Furthermore, the authors investigated the influence of NaCl, which induced electrostatic repulsions in the poly(methacrylic acid) (PMAA) chains, resulting in the formation of small micelles.

Later, Laschewsky's group reported the RAFT polymerisation of butyl acrylate or 2-ethylhexyl acrylate (EHA), and FDMA using a PEO macromolecular chain transfer agent. The resulting linear amphiphilic diblock and triblock copolymers were self-assembled using method 5 at room temperature and at 70 °C.⁷⁰ In both cases, the polymers formed stable micellar aggregates for a prolonged period of time. However, fluorinated nano-domains in the micelle cores were not observed, possibly because of their size.⁷⁰

Later, the same authors reported the synthesis and aqueous self-assembly of the PEHA-*b*-POEGA-*b*-PFDA triblock copolymer using method 5.⁷¹ In contrast to their previous study, this triblock copolymer self-assembled into unusual "soccer ball-like" multicompartiment micelles due to the incompatibility of the POEGA and PFDA hydrophobic blocks (Fig. 6). In 2010, they explored the self-assembly of a series of POEGA-*b*-PFDA, POEGA-*b*-PBA-*b*-PFDA and PEHA-*b*-POEGA-*b*-PFDA block copolymers.⁷² The block copolymers were self-assembled in water

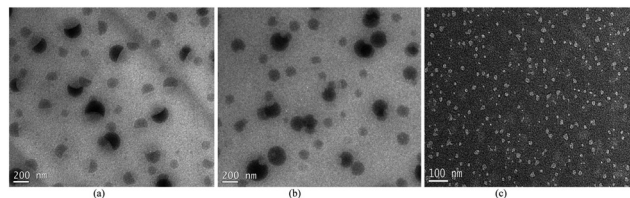


Fig. 5 TEM pictures of PMMA-*b*-PFDPMA diblock copolymers in $CHCl_3$ (a), THF (b), and TFT (c) solutions. Light area = PMMA, dark areas = PFDPMA. Reproduced with permission from ref. 65. Copyright 2012 RSC.

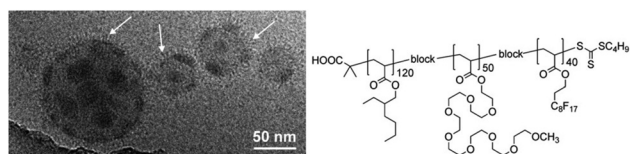


Fig. 6 Cryo-TEM micrograph of PEHA-*b*-POEGA-*b*-FDA triblock copolymer self-assembled in water. Reproduced with permission from ref. 71. Copyright RSC 2009.

using methods 3 and 6. Whereas only spherical aggregates without phase segregation were observed for the POEGA-*b*-PFDA diblock copolymer, unprecedented multicompartiment morphologies, such as “patchy double micelle” and larger “soccer ball” structures, were identified for POEGA-*b*-PBA-*b*-PFDA and PEHA-*b*-POEGA-*b*-PFDA triblock copolymers.⁷²

The concept was further investigated by Gao *et al.* for PAA-*b*-PCOEMA-*b*-PFDMA or *Pt*BA-*b*-PCOEMA-*b*-PFDMA (COEMA = 2-cinnamoyloxyethyl methacrylate, *t*BA = *tert*-butyl acrylate) triblock copolymers.⁷³ Using method 1, almost all triblock copolymers generated cylindrical micelles at room temperature in different TFT/alcohol binary mixtures. The sole exception was the triblock copolymer with the lowest PFDMA mass fraction and the highest soluble block mass fraction, which formed a mixture of cylindrical and spherical micelles. All the micelles possessed a PFDMA core, a PCOEMA shell, and a PAA or *Pt*BA corona. TEM images indicated that the PFDMA chains in the core were almost fully stretched and that the PCOEMA chains in the PAA/PCOEMA/PFDMA cylindrical micelles were radially compressed. More exotic morphologies and shapes resembling triangles, rhombuses, squares as well as ring, eye- and racket-shaped aggregates were also reported later by the same authors on similar BCs.⁷⁴ The authors suggested that the formation of cylindrical morphologies was driven by the fluorinated-block yielding cylinders with abnormal shell thicknesses. The singular LC property of PFDMA copolymers was used again by Manners and co-workers in P2VP-*b*-PFDMA (P2VP = poly(2-vinylpyridine) LC diblock copolymers prepared by sequential anionic polymerisation.⁷⁵ In a first attempt, using method 1, cylindrical micelles governed by the crystallinity of the fluorinated block were obtained with relatively broad length distributions. Yet, using a fragmentation *via* sonication followed by annealing approach, the authors were able to produce monodisperse cylindrical micelles with controlled lengths. The broad length distribution likely caused by the low energy barrier of nucleation and fast growth process was later addressed by the addition of small molecules to a solution of similar block copolymers (see Fig. 7), inducing supramolecular interactions.⁷⁶ These interactions resulted in the formation of hierarchical nanostructures with precise control over their size *via* a three-step assembly strategy (Fig. 7). The observed morphologies were linear, branched, segmented, hairy plate-like, and star-like nanostructures.

2.1.11. Perfluoroalkyl ethyl methacrylate (FEMA). To date, only one article reported the self-assembly of PFEMA-

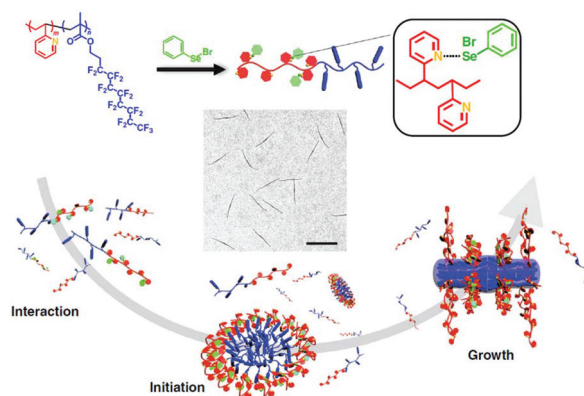


Fig. 7 Chemical structure and schematic representation of the P2VP-*b*-PFDMA block copolymer with a detailed cylindrically driven 3-step growth process. Interaction: PhSeBr initiators form complexes with pyridyl groups. Initiation: these interactions result in a less soluble complex, which tends to aggregate, resulting in PFMA chains having a higher propensity to form oligomeric aggregates with LC cores. Growth: formed complexed aggregates serve as seeds for the growth of free monomeric polymer chains through the LC ordering effect. Adapted with permission from ref. 76. Copyright Springer Nature 2019.

based copolymers. Li *et al.* prepared P(MMA-*co*-MAA)-*b*-PFEMA diblock copolymers by RAFT polymerisation and self-assembled them in water using method 3.⁷⁷ The triphilic copolymers (hydrophilic, lipophilic, and fluorophilic due to MAA, MMA, and FEMA, respectively) displayed nanostructures, such as spheres and short worms that evolved into worms, tapered worms, and finally to nail-shaped structures, as the water content increased from 10 to 80 vol%. This morphological transition upon the addition of water was ascribed to the increase in interfacial tension between the core-forming block and the solvent.

2.1.12. Iodotetrafluorophenoxy methacrylate (IFPMA). This peculiar iodine atom-bearing fluorinated monomer was investigated to examine the effect of halogen-interactions⁷⁸ on the formation of hierarchical morphologies. Vanderkooy and Taylor described an attractive method based on non-covalent halogen bonding interactions as the driving force for the solution self-assembly of fluorinated copolymers.⁷⁹ First, a PEG-*b*-PDMAEMA diblock copolymer was synthesised by ATRP as the halogen-bond acceptor, then PEG-*b*-PIFPMA diblock copolymer was prepared by RAFT as the halogen-bond donor. Mixing the donor and the acceptor resulted in the formation of higher-order structures in organic solvents as well as in water.

2.1.13. 2-(Trifluoromethyl)acrylic acid (MAF) and its ester. 2-(Trifluoromethyl)acrylic acid (MAF) and its esters do not homopolymerise *via* radical homopolymerisation. They however readily copolymerise with more electron-rich olefins, such as vinyl acetate.^{80–82} Falireas *et al.*⁸³ recently prepared amphiphilic diblock terpolymers composed of a PNIPAM or PDMA (DMA = *N,N*-dimethyl acrylamide) hydrophilic block and a hydrophobic poly(MAF-TBE-*alt* Vac) block (MAFTBE = *tert*-butyl-2-(trifluoromethyl)acrylate) *via* sequential RAFT polymerisation. Hydrolysis of the ester groups produced double

hydrophilic diblock terpolymers endowed with pH-responsiveness (and thermoresponsiveness for the PNIPAM-based BCP). Both the hydrolysed and the non-hydrolyzed BCP were shown to form vesicular structures by self-assembly.

2.1.14. Mixture of monomers. In addition to copolymers containing a single fluorinated monomer family, other copolymers composed of different fluorinated moieties were also investigated, leading to simple micelles or less well-defined morphologies. For instance, Hwang *et al.* reported the preparation of amphiphilic semifluorinated block copolymers composed of PDMAEMA as the hydrophilic block and PDHFOMA or PTHFOMA blocks as the fluorinated block.⁸⁴ The size of the micelles was shown to be influenced by the copolymer composition, the pH, and the temperature. Niu *et al.* also reported the self-assembly of complex multiblock architectures consisting of a fluorosilicone block extended with PMMA and polymers of various fluorinated methacrylates, such as TriFEMA, HexFBMA, OFPMA, and FDMA.⁸⁵ The self-assembly behavior was difficult to predict and led to pure micelles or unimers, depending on the solvent used.

Mugemana *et al.* studied a number of fluorinated amphiphilic star block copolymers starting from tris(benzyltriazolylmethyl)amine and composed of diblocks of polypentafluorostyrene (PPFS), PHepFBA, or PTHFOA and hydrophilic *p*-oligo(ethylene glycol) styrene (POEGSt) or POEGMA.⁸⁶ Spherical aggregates with diameters ranging from 20 to 50 nm were the main structures observed for PFS-, HepFBA- and PTHFOA-containing copolymers. Increasing the mass fraction of PHepFBA led to the formation of unilamellar and multilamellar vesicles.

2.2. Polymerisation-induced self-assembly (PISA)

Polymerisation-induced self-assembly (PISA) has emerged as an extremely effective technique for preparing self-assembled polymer aggregates with controlled and defined morphologies at high solid contents with high reproducibility.^{87–97} Under the PISA process, a solvophilic polymer precursor dissolved in a solvent is extended with a solvophobic polymer. As polymerisation proceeds, chain extension leads to the formation of an “amphiphilic” block copolymer that self-assembles into colloidally stable nano-objects. When combined with the RAFT polymerisation technique (the most commonly used RDRP technique in PISA), it allows the formation of diverse morphologies, such as spheres, worm-like micelles and vesicles. So far, most PISA protocols have used RAFT polymerisation in dispersion or emulsion and involved hydrogenated acrylic monomers. However, a few articles report the use of fluorinated monomers in the PISA process.

2.2.14. Alkyl perfluorinated (meth)acrylate. In 2008, Howdle pioneered the use of a fluorinated macro-RAFT agent for the surfactant-free polymerisation of MMA in $scCO_2$.⁹⁸ A PDHFOMA RAFT macro-CTA was chain extended with MMA. Polymerisation exhibited excellent control under dispersion polymerisation conditions and resulted in well-defined core-shell spherical particles (1–5 μ m). Xu *et al.* revisited this study and used fluorinated methacrylate (with a pendant $-C_6F_{12}H$ group) to polymerise MMA *via* PISA protocols in $scCO_2$.⁹⁹

Spherical nanoparticles with different sizes and polydispersity were obtained. Armes and coworkers reported the morphological transition of PMAA-*b*-PBzMA (BzMA = benzyl methacrylate) block copolymer nanostructures upon chain extension with TriFEMA in ethanol under dispersion polymerisation conditions (Fig. 8).¹⁰⁰

The same group used the same concept with PMAA and PDMAEMA RAFT macro-CTAs that they chain-extended with TriFEMA.¹⁰¹ TEM images indicated that well-defined spherical nanoparticles were produced in both cases. In contrast, a shorter PDMAEMA macro-CTA led to the formation of spheres, which evolved into worms and polydisperse vesicles, depending on TriFEMA conversion. This evolution of the self-assembled morphologies was caused by the gradual reduction in the molecular curvature of the growing copolymer chains. The Armes group also performed detailed SAXS studies to determine the effective particle density, steric stabiliser layer thickness, as well as the volume-average number of a series of PGMA-*b*-PTriFEMA nanoparticles synthesised by PISA (PGMA = poly(glycerol monomethacrylate)).¹⁰² In addition, they also prepared similar but transparent diblock copolymer nanoparticles (PSMA-*b*-PTriFEMA) in *n*-alkane at different concentrations (PSMA = poly(stearyl methacrylate)). Transparency was due to the matching refractive indexes of PTriFEMA and *n*-alkane.^{103,104} Such particles are used in smart (such as anti-reflective) coatings. Similarly to the work reported by Armes and co-workers,¹⁰¹ Li's group reported a PISA process using a PMAA macro-CTA and PTriFEMA as the core-forming fluorinated polymer.¹⁰⁵ TriFEMA was also recently used in the PISA formulation of polymer nano-objects for cellular take up and tracking *via* ^{19}F MRI.¹⁰⁶ Detrembleur *et al.* used aqueous PISA for the preparation of transparent superhydrophobic coatings.¹⁰⁷ Hydrophilic PMAA macro-CTA was synthesised and chain-extended with FDMA and *n*-butyl acrylate to produce stable fluorinated particles, which were successfully spin-

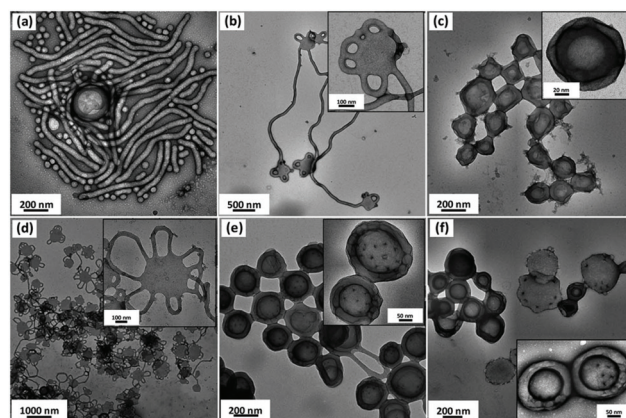


Fig. 8 Representative morphologies obtained after dispersion PISA of TriFEMA in ethanol. (a) PMAA₇₀-*b*-PBzMA₁₀₀-*b*-PTriFEMA₁₀₀; (b) PMAA₇₀-*b*-PBzMA₂₀₀-*b*-PTriFEMA₂₀₀; (c) PMAA₇₀-*b*-PBzMA₇₀-*b*-PTriFEMA₂₂₃; (d) PMAA₇₀-*b*-PBzMA₁₉₁-*b*-PTriFEMA₆₀; (e) PMAA₇₀-*b*-PBzMA₂₄₃-*b*-PTriFEMA₆₀; (f) PMAA₇₀-*b*-PBzMA₂₇₃-*b*-PTriFEMA₆₀. Reproduced with permission from ref. 100. Copyright 2014 RSC.

coated with fillers to produce superhydrophobic transparent coatings after further treatment. Ma's group reported the *ab initio* emulsifier-free emulsion copolymerisation of a mixture of monomers including HexFBMA. However, they did not provide enough evidence of the successful copolymerisation of the monomer mixture or of efficient chain extension of the PDMAEMA-*b*-PHexFBA macro-CTA.^{108,109} The same group also reported the formation of stabilised spherical particles in ethanol using PAA and PHexFBMA as the hydrophilic block and fluorophilic/hydrophobic block respectively.^{110,111} Spherical core-shell latex particles were formed, as determined by TEM and DLS studies. The size of these latex particles could be increased by increasing the pH. Huo *et al.* reported the seeded RAFT dispersion polymerisation of THFOMA using PDMAEMA-*b*-PBzMA macro-CTA already self-assembled into micelles, worms and vesicles.¹¹² Phase segregation of PTHFOMA and PBzMA block copolymers was evidenced by the formation of compartmentalized nanostructures. An abundant variety of segregated morphologies were observed, such as patchy, ribbon-shell and raspberry-like micelles (Fig. 9). The morphology evolution of these multi-compartment micelles (MCM) was controlled by the lengths of the PBzMA and PTHFOMA blocks. A series of PISA formulations based on semi-fluorinated methacrylates with different fluorinated side-chain lengths (C₄F₉ NFHMA, C₆F₁₃ THFOMA, C₈F₁₇ FDMA) was reported by the same team.¹¹³ Among their findings, these authors highlighted that only spheres could be prepared when PTHFOMA was used as the core forming block. Elongated cylindrical micelles could be obtained when FDMA was used, presumably because of the liquid crystalline nature of FDMA.

The same authors also reported the one-pot PISA synthesis of PDMA-*b*-PBzMA-*b*-PFDMA triblock copolymers in ethanol (Fig. 10a).¹¹⁴

Upon variation of the chain lengths of PBzMA and PFDMA (also called PFMA), the authors observed different morphology evolutions, which were attributed to the interplay of the hydrophobic interactions between the PBzMA blocks, the lipophobic interaction, and the LC ordering of the PFDMA blocks

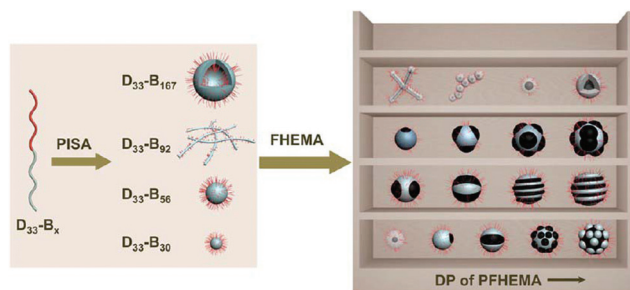


Fig. 9 (Left) Schematic representation of the PISA process and resulting morphologies obtained during the preparation of PDMAEMA-*b*-PBzMA micelles, worm-like and vesicles seeds. (Right) Compartmentalized nanostructures with a large variety of morphologies as a function of DP of PFHEMA (coined PTHFOMA in the text). Color code: D (red, PDMAEMA), B (grey, PBzMA), and H (black, PTHFOMA). Reproduced with permission from ref. 112. ACS 2017 Copyright.

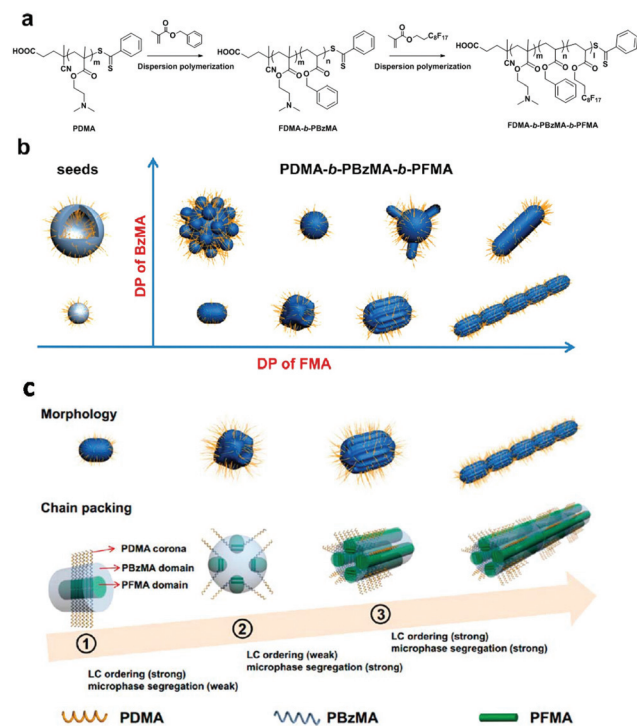


Fig. 10 (a) Synthesis route utilized for the preparation of PDMA-*b*-PBzMA-*b*-PFDMA triblock copolymers. (b) Schematic representation of the obtained morphologies as a function of BzMA and PFDMA (FMA) degree of polymerisation (DPn). (c) Proposed mechanism for the formation of LC ordered morphologies with increasing PFDMA block length: PDMA₃₃-*b*-PBzMA₅₈-*b*-PFDMA_{16,30,62,120} (from left to right). Adapted with permission from ref. 114. ACS 2017 Copyright.

(Fig. 10b and c). This system was later optimized and explored in detail by the same group.^{115–117} Recently, ICAR ATRP under PISA conditions was also used to prepare organic-inorganic hybrid nanoparticles (ICAR = initiators for continuous activator regeneration).¹¹⁸ The fluorinated block (PFDMA) was used to tune the solubility of the copolymers, while glycidyl methacrylate (GMA) provided reactive epoxy groups that were later used for surface modification. By modulating the solid content as well as the GMA/THFOMA molar ratio, various morphologies, such as spheres and short worms, were achieved.

2.2.15. Pentafluorophenyl (meth)acrylates (PFP(MA)). Perfluorinated alkyl methacrylates have been relatively well investigated, probably because they offer the possibility of modulating their hydrophobicity/fluorophilicity ratio *via* varying the length of the fluorinated chain. In comparison, pentafluorophenyl methacrylates were more rarely studied. However, they have gained attention because of the selective reactivity of the *para* position, providing an attractive and efficient tool for chemical post-modification.^{119–122} Indeed, every type of thiol (primary, secondary, and tertiary as well as aliphatic and aromatic thiols) has been shown to affect the substitution of the fluorine atom on the *para* position, while the pentafluorophenyl activated ester group is known to efficiently react with amines to form amides. The PISA of pen-

tafluorophenyl methacrylates was pioneered by the Lowe group in 2015, who reported the preparation of fluorinated poly-methacrylate copolymer self-assembled nanoobjects *via* RAFT dispersion polymerisation in ethanol.¹²³ Aggregates with common morphologies, such as spheres, worms, and vesicles, were obtained. These particles were then chemically modified using a thio-sugar. This modification resulted in identical morphologies or minor changes, such as mixed phases of spheres and worms. Following this methodology, the same group also prepared other fluorinated soft nanoparticles of various morphologies.¹²⁴ Using a copolymer of stearyl methacrylate (SMA) and pentafluorophenyl methacrylate (PFPMMA), they performed RAFT dispersion polymerisation of 3-phenylpropyl methacrylate (PPMA) in *n*-octane or *n*-tetradecane. TEM images showed typical PISA morphologies. The reactive pentafluoro methacrylate units were then modified into acrylamides *via* an acyl substitution reaction with a primary amine. Using a similar approach but by using *para*-fluoro substitution with thiols, Roth and co-workers prepared cross-linked particles,¹²⁵ or induced morphological transitions.¹²⁶ In this latter example, PEGMA-*b*-PFBMA diblock copolymers prepared *via* RAFT dispersion polymerisation in ethanol generated either spherical or worm-shaped morphologies that were modified, post-synthesis, with a selection of 15 different thiols through thiol-*para*-fluoro substitution reactions in the nano-object cores. Depending on the choice of thiol, spherical nano-objects underwent an order-disorder transition to form unimers, increased in size, or underwent an order-order transition to form worm-shaped nano-objects. These morphological transitions were ascribed to the modification of the packing parameters caused by the change in the solvophobicity brought about by the grafted thiol moieties.

3. Poly(fluorinated styrene)-based copolymers

The self-assembly of fluorinated styrene-based BCP was pioneered by the Laschewsky group with an ABC poly(4-methyl-4-(4-vinylbenzyl)morpholin-4-ium chloride)-*b*-polystyrene-*b*-poly(pentafluorophenyl 4-vinylbenzyl ether) (PVB_M-*b*-PS-*b*-PVBFP) linear triblock copolymer.¹²⁷ This triblock copolymer was prepared by quaternization of a poly(vinylbenzyl chloride)-*b*-PS-*b*-PVBFP precursor (synthesised by RAFT polymerisation) with *N*-methylmorpholine. The triblock copolymer was dispersed in a dioxane/water binary mixture and self-assembled using method 7. Cryo-TEM images revealed the presence of 20–30 nm multicompartment micelles with cores segregated into nanometer-sized compartments containing small fluorocarbon-rich domains coexisting with the continuous hydrocarbon-rich region (Fig. 11).

In another report, the complexation of polyanionic blocks with multivalent counter cation was used to obtain polyion complex (PIC) micelles that underwent local intra-micellar phase separation.¹²⁸ Polystyrene (PS) and poly(2,3,4,5,6-pentafluorostyrene) (PPFS) were employed as the third hydrophobic

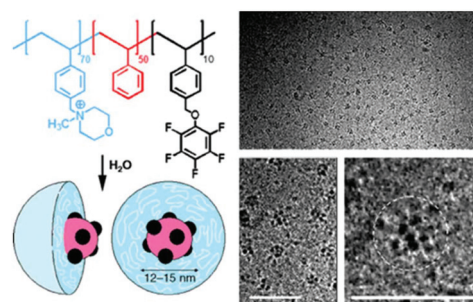


Fig. 11 Structure of PVB_M-*b*-PS-*b*-PVBFP triblock copolymer, cryo-TEM images, and schematic representation of multicompartment micelles arising from self-assembly in water. The corona of the micelles is not visible. The scale bars correspond to 50 nm. Adapted with permission from ref. 127. Wiley-VCH 2005 Copyright.

block in PAA-*b*-PMA-*b*-PS and PAA-*b*-PMA-*b*-PPFS. Equal molar amounts of these two triblock copolymers were dissolved in pure THF. A diamine (1 : 1 molar ratio with PAA) was added to complex the PAA block and induce the formation of the PIC micelle. In the next step, the addition of water (THF : water = 1 : 2) triggered the formation of cylindrical micelles. The incompatibility of PS and PPFS resulted in nano-phase separation, producing multicompartment micelles with pronounced undulations along the cylinder surfaces.¹²⁸

In 2008, the Davis' group reported the RAFT synthesis of a pH-responsive amphiphilic PDMAEMA-*b*-PPFS block copolymer.¹²⁹ Micelle formation, in water using method 1, was investigated by fluorescence spectroscopy, static light scattering (SLS), DLS, and TEM. DLS and SLS measurements revealed that the diblock copolymers formed spherical micelles with large aggregation numbers, where the dense PPFS cores were surrounded by PDMAEMA chains. The hydrodynamic radii, R_h , of these micelles at pH 2–5 were larger, as the protonated PDMAEMA segments swelled the micelle corona. R_h decreased as the pH increased due to increasing hydrophobicity. Nonetheless, the radius of gyration (R_g) remained pH independent, as the PPFS core was not pH-responsive. In a parallel study, the same group synthesised well-defined fluorinated brush-like amphiphilic diblock copolymers of PPEGMA and PPFS by ATRP and self-assembled those copolymers using method 1.¹³⁰ The hydrodynamic radius (R_h) of the micelles in aqueous solution was in the nanometer range, regardless of the polymer concentration. Diblock copolymers with longer PPEGMA block (DP = 19) formed micelles with smaller R_h and lower aggregation numbers. Interestingly, an increase in temperature induced the comb-like PEG segments in the corona to dehydrate and shrink (lower critical solution temperature (LCST) behaviour), leading to the formation of micelles with larger aggregation numbers.¹³⁰ The same authors also reported the synthesis, micelle formation, and bulk properties of semifluorinated amphiphilic PEG-*b*-PPFS-*g*-POSS (POSS: polyhedral oligomeric silsesquioxane) copolymers.¹³¹ The synthesis of the PEG-*b*-PPFS diblock copolymer was achieved *via* ATRP using a poly(ethylene glycol)-based macroinitiator.

Subsequently, a fraction of the reactive fluorine atoms on the *para* position of the PPFS units was replaced with amino-functionalised POSS through an aromatic nucleophilic substitution reaction. The products, PEG-*b*-PPFS and PEG-*b*-PPFS-*g*-POSS, were self-assembled in aqueous solutions using method 3. The CMC (critical micelle concentration) of these polymers decreased concomitantly with the number of POSS particles grafted per copolymer chain. Wooley's group¹³² prepared, *via* a relatively complex synthesis procedure consisting of self-condensing ATRP of an inimer, 1-(40-(bromomethyl)-benzyloxy)-2,3,5,6-tetrafluoro-4 vinylbenzene, amphiphilic hyperbranched fluoropolymers that formed nanometric micelles. Tan *et al.*¹³³ synthesised a series of amphiphilic copolymers by radical copolymerisation of sodium 2-acryamido-2-methylpropanesulfonate and styrene derivatives with a fluorocarbon side chain (3,3,4,4,5,5,6,6,7,7,8,8,8-tridecafluoro-1-octanol). Their self-assembly in aqueous solution using method 1 indicated that the self-assembly and surface activity depended on the fluorocarbon content of the copolymer. Since 2019, these fluorinated copolymers have gained attention, especially for preparation of internally ordered morphologies, such as cubosomes and nanotubes.¹⁹ Lv *et al.*¹³⁴ prepared various self-assembled morphologies of PDMA-*b*-(P(*S-alt*-PPFS)) block copolymers prepared by PISA using a PDMA (polydimethylacrylamide) macro-CTA. At DP < 300 for the P(*S-alt*-PPFS) block, common morphologies (spheres, worms and vesicles) were observed. When higher DPs (428 or 582) were targeted, cubosomes with *Im3m* and *P6mm* mesophases were obtained. The formation of such morphologies was attributed to both high solid contents and the short PDMA stabiliser block, facilitating inelastic collision between particles, resulting in the formation of higher order morphologies. The addition of a small fraction of co-solvent at high monomer conversions (acting as a plasticizer) facilitated chain mobility and the morphological transition. The addition of a co-solvent to promote plasticity was also used to prepare BCP nanotubes.¹³⁵ PDMA-*b*-PPFS BCP morphologies were prepared by performing PISA in ethanol, and DMF was added to promote nanotube formation (Fig. 12). Through several experiments, this study showed that nanotube formation was governed by T_p (polymerisation temperature) and T_{sg} (glass transition temperature) of the solvated cores. The formation of nanotubes was highly favoured when T_p was lower than or close to T_{sg} .

4. Poly(perfluoropolyether)-based copolymers (PFPE)

4.1. PFPE-based miktoarm triblock copolymers

The ABC miktoarm (μ -ABC) star terpolymer architecture provides a versatile and powerful route to multicompartment micelles. Because of the mandatory convergence of three blocks at a common point, the miktoarm star architecture suppresses the formation of the default core/shell/corona "onion-like" arrangement often adopted by linear ABC triblock terpolymers. This promotes segregation of all three mutually immis-



Fig. 12 (A) Chemical structure of PDMA-*b*-PPFS block copolymer prepared by RAFT PISA. (B) Morphological evolution of PDMA-*b*-PPFS block copolymer through the PISA process with $T_p \approx T_{sg}$ or $T_p < T_{sg}$. (C) and (D) Nanotube morphologies obtained for PDMA₂₉-*b*-PPFS₁₈₀ and PDMA₂₉-*b*-PPFS₂₀₀ at 30% w/v solid content in 5% DMF/ethanol (T_p and $T_{sg} = 65$ °C). Adapted with permission from ref. 135. ACS 2020 Copyright.

cible polymer chains at their contact point. In 2004, Lodge *et al.*¹³⁶ reported the observation of multicompartment micelles prepared from a miktoarm star polymer comprising a water-soluble poly(ethylene oxide) (PEO) arm and two hydrophobic immiscible components, poly(ethylene) (PEE) and poly(perfluoropropylene oxide) (PFPO). These μ -(PEE)(PEO) (PFPO) star triblock copolymers, abbreviated as μ -EOF, were prepared using two successive anionic polymerisation steps and one polymer-polymer coupling reaction.¹³⁷ Different types of multicompartment micellar structures were identified in dilute aqueous solution, depending on the composition of the μ -EOF star triblock copolymers,¹³⁸ as revealed by cryogenic transmission electron microscopy (Fig. 13). The observed micellar structures were generally correlated with the O (PEO) corona size and the relative lengths of the E (PEE) and F (PFPO) blocks. The strong incompatibility of the three poly-

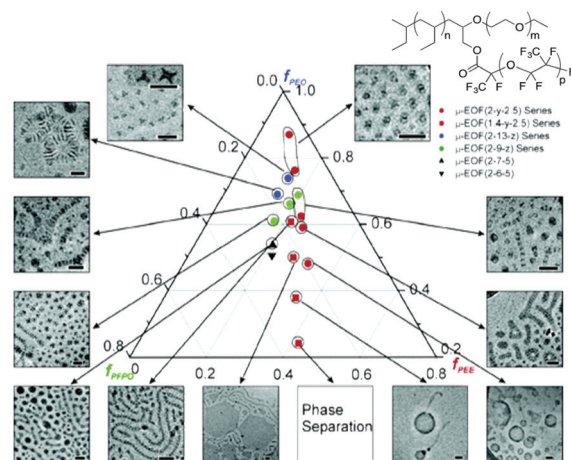


Fig. 13 Multicompartment micelle morphology diagram for μ -EOF miktoarm star terpolymers in dilute aqueous solution as a function of composition. f_{PEE} , f_{PEO} , and f_{PFPO} are the volume fractions of the PEE, PEO, and PFPO blocks, respectively. They are designated μ -EOF(x - y - z), where x , y , and z represent the E, O, and F block molar masses, respectively, in kD. Reproduced with permission from ref. 138. Copyright 2006 ACS.

meric components drove the formation of segregated micelle cores even at modest molar masses. The extreme hydrophobicity of the F block placed the system in the superstrong segregation regime¹³⁹ within which the interfacial tension is so large that the minority core-forming block is essentially completely extended and the interfacial area per chain is minimized. Upon decreasing the length of the O block, the resulting micelles evolved from “hamburger” micelles to segmented worms and ultimately to nanostructured bilayers and vesicles (Fig. 13). When the F block was the minority component, segmented ribbons, Y-junctions, and networks were preferred.

A longer F block, compared with the E block, resulted in the formation of novel morphologies, such as raspberry-like micelles and multicompartimentalised worms.¹⁴⁰ Solvent selectivity was also shown to be an efficient way to reach various micellar morphologies with miktoarm star μ -EOF micellar systems. By incorporating a good solvent for the E block (e.g. THF) into aqueous dispersions of a μ -EOF block, the micellar structure evolved from multi-compartment disks to core-shell corona worms, spheres and finally to mixed corona (E + O) oblate ellipsoidal micelles with increasing THF content.¹⁴¹ Using a μ -ABC/AB blend, the same authors reported the formation of “hamburger” micelles from EO diblock copolymers (forming spherical micelles) and μ -EOF miktoarm star terpolymers (forming segmented worm-like micelles).¹⁴² This morphological evolution most probably occurred *via* the collision/fusion/fission mechanism, whereby the long μ -EOF segmented worm-like micelles first fused with EO spherical micelles, followed by fission, giving progressively shorter micelles, which finally evolved into more stable hamburger-like micelles. To date, the use of multicompartment micelles for nanotechnology applications that utilize their inherent storage and release capacities remains limited. The Lodge group has demonstrated the possibility of using μ -EOF-based multicompartment micelles to solubilise two distinct hydrophobic dye molecules within two separate nano-sized compartments.¹⁴³ Crucially, these findings indicate that there is little relationship between the distinct solubilisation efficiencies and therefore simultaneous or sequential storage and release of two different hydrophobic payloads could be possible.

4.2. PFPE-based miktobrush terpolymers

In 2016, Hillmyer's group reported the aqueous self-assembly of μ -A(BC)*n* miktobrush terpolymers synthesised using RAFT polymerisation.¹⁴⁴ In this system, the A block (attached to the R-group of the RAFT CTA) was hydrophilic PEO (O). The B block was hydrophobic PMCL (C), and the C block was hydrophobic/oleophobic PFPO (F), both in the form of a macromonomer polymerised using the PEO-modified CTA. The aqueous self-assembly of μ -O(CF)*n* miktobrush terpolymers was characterized using DLS and cryo-TEM. The first terpolymer investigated ($f_{\text{PEO}} = 0.63$, $f_{\text{PMCL}} = 0.28$, $f_{\text{PFPO}} = 0.09$) formed hamburgers and evolved over time to raspberry-like micelles (likely due to the large volume fraction of PEO). This transition seemed to be attributed to partial solvation of PEO

by PMCL chains, which induced a larger volume fraction of PEO. Within the hamburger micelles, the PMCL chains formed the “buns” around an oblate PFPO core disk, thereby decreasing the interfacial penalty between the PFPO domains and the solvated PEO blocks. These findings are broadly consistent with their previous findings on μ -EOF and μ -EOC miktoarm star terpolymer systems.^{136,138,144} The μ -O(CF) terpolymer ($f_{\text{PEO}} = 0.57$, $f_{\text{PMCL}} = 0.35$, $f_{\text{PFPO}} = 0.08$) formed multilamellar vesicles or polymersomes with nanoscopic periodicity within their bilayer, because of dispersed PFPO domains within the PMCL matrix.

4.3. PFPE-based linear block copolymers

Thüneman *et al.*¹⁴⁵ synthesised a symmetrical linear ABCBA pentablock copolymer consisting of (A) PEO, (B) poly(γ -benzyl L-glutamate) (PBLG), and (C) a perfluoropolyether (PFPE, Fluorolink® C). The diblock copolymer PEO-*b*-PBLG was synthesised by ring-opening polymerisation of the *N*-carboxy anhydride of γ -benzyl-L-glutamate using ammonium chloride-functionalised PEO as the macroinitiator. In a second step, the PEO-*b*-PBLG diblock was covalently coupled to an α,ω -dicarboxyl-PFPE *via* a carboxyl-amine reaction. The different blocks were highly immiscible and formed two-compartment cylindrical micelles in aqueous solution. In 2006, Lodge *et al.*¹⁴⁶ reported the first example of a coil-coil nonionic diblock copolymer adopting a flat disk morphology. The diblock copolymer was synthesised through the coupling reaction of hydroxy-terminated 1,2-polybutadiene and acid-chloride-end-functionalised PFPE (Krytox® 157-FSH). Both blocks were atactic, noncrystalline, and flexible (low T_g). Micellization was performed in bis(2-ethylhexyl) phthalate, selective solvent for polybutadiene. The self-assembled thin disk micelles had radii ranging from 20 to 150 nm and a core thickness of approximately 10 nm. The adopted morphology was clearly the result of an unusually significant interfacial tension between the fluoropolymer and the solvated polybutadiene block. The same authors studied the self-assembly of two PFPE-based triblock copolymers, BOF and FOF.^{147,148} First, a hydroxy-terminated poly(1,2-butadiene)-*b*-poly(ethylene oxide) (BO) diblock copolymer was synthesised by two successive living anionic polymerisations. Carboxylic acid end-capped poly(perfluoropropylene oxide) (PFPO-COOH) was converted into the acid chloride derivative by reaction with oxalyl chloride. The BOF triblock was obtained by coupling the hydroxy end-functionalised BO with the acid chloride end-functionalised PFPO. FOF was synthesised by reacting α,ω -dihydroxy-PEO with acid chloride end-functionalised PFPO. Aqueous gels formed from these polymers at concentrations ranging from 10 to 50 wt% were investigated using cryogenic scanning electron microscopy (cryo-SEM) and SANS. The cryo-SEM micrographs revealed significant differences among the morphologies of the resulting gels, depending on the end-block used (Fig. 14). The FOF copolymer formed networks by aggregation of the end-blocks, but the PFPO blocks tended to adopt disk-like or even sheet-like structures. This was attributed to the significant interfacial tension of PFPO with water, consistent with the superstrong

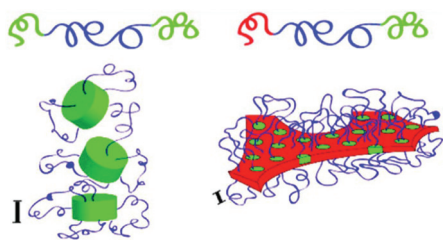


Fig. 14 Schematic representations showing the dependence of the network morphology on the end-blocks. 1,2-Polybutadiene, poly(ethylene oxide), and poly(perfluoropropylene oxide) are shown in red, blue, and green, respectively. The scale bars represent 5 nm. Adapted with permission from ref. 147. Copyright 2010 ACS.

segregation regime. The heterotelechelic BOF terpolymers formed an intricate bicontinuous open-cell foam, with cell sizes around 500 nm with walls composed of PFPO disks embedded in PB sheets. These different network structures illustrate the potential of using end-block chemistry to control both the morphology and the physical properties of fluorinated polymer gels.

Qiao *et al.* reported the synthesis of a perfluoropolyether-*b*-poly(*t*-butyl acrylate) (PFPE₁₈₀₀-*b*-PtBA₈₄₀₀) diblock copolymer in two steps.¹⁴⁹ A mono-hydroxy PFPE was reacted with 2-bromoisobutryl bromide to form a macroinitiator containing a terminal bromine moiety. This ATRP macroinitiator was then used to polymerise *t*-butyl acrylate (*t*BA). Self-assembly of the resulting PFPE₁₈₀₀-*b*-PtBA₈₄₀₀ diblock copolymer was conducted in benzene (selective solvent of PtBA). DLS analyses revealed the formation of 400 nm monodisperse micelles. The diblock copolymer was also used to prepare honeycomb patterned films on both planar and non-planar surfaces *via* the breath-figure technique using a static casting system.¹⁴⁹ Lopez *et al.* reported the synthesis of a PEG₂₀₀₀-based amphiphilic triblock copolymer containing a PFPE₁₂₀₀ central core that was synthesised by copper(i)-catalyzed alkyne-azide cycloaddition (CuAAC) between a telechelic alkyne PFPE and a PEG-azide.¹⁵⁰ The PEG₂₀₀₀-*b*-PFPE₁₂₀₀-*b*-PEG₂₀₀₀ triblock copolymer self-assembled into spherical micelles in aqueous solution with diameters of 10–20 nm. In 2007, Lodge *et al.* synthesised two polylactide-*b*-poly(perfluoropropylene oxide) diblock copolymers *via* coupling of acid chloride end-functionalised PFPOs and hydroxy-terminated PLAs.¹⁵¹ The solubility of these materials in scCO₂ was measured using a variable-volume high-pressure cell. At a concentration of 1 wt%, the diblock copolymers were found to be soluble at modest pressures (<500 bar) over the temperature range of 30–65 °C. The size of the resulting micelles in scCO₂ was characterized by high-pressure-DLS. These measurements indicated the formation of predominantly small, spherical micelles for PLA₄₀₀₀-*b*-PFPO₆₀₀₀ and large aggregates with hydrodynamic radii of 100 nm for PLA₅₀₀₀-*b*-PFPO₄₀₀₀. Vesicles were formed by kinetically trapping the aggregates in CO₂ through vitrification of the PLA cores and re-dispersing them in a PFPO selective solvent. This vesicles were later used in microfluidic devices,

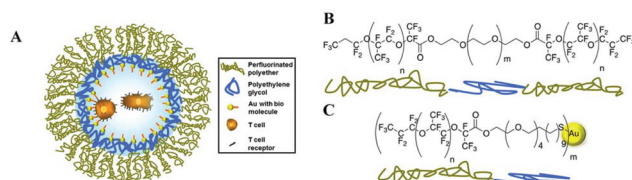


Fig. 15 (A) Schematic representation of a nanostructured and specifically biofunctionalised drop of a water-in-oil emulsion as a 3D APC analogue. (B and C) Structures of the PFPE-*b*-PEG-*b*-PFPE triblock copolymer and PFPE-*b*-PEG-gold diblock surfactant, respectively. Reproduced with permission from ref. 153. Copyright 2013 ACS. Notice to reader: further permissions related to the material excerpted from <https://pubs.acs.org/doi/10.1021/ja311588c> should be directed to the ACS.

which could find applications for *in vitro* translation, encapsulation and incubation of cells.¹⁵² Spatz *et al.*¹⁵³ developed a novel approach to form biofunctionalised droplets of water-in-oil emulsions with the potential to serve as 3D APC (antigen-presenting cells) surrogates (Fig. 15). The PFPE-*b*-PEG-*b*-PFPE triblock copolymer (Fig. 15B) was obtained using a one-step condensation reaction between PEG₆₀₀-diol and PFPE₂₅₀₀-dicarboxylic acid. PFPE-*b*-PEG-gold diblock surfactant (Fig. 15C) was synthesised using a one-step condensation reaction between PFPE₇₀₀₀-carboxylic acid and (11-mercaptoundecyl)-tetra(ethylene glycol)-functionalised gold nanoparticles. Two alternative approaches were adopted to test how efficiently the gold nanoparticles inside the droplets could serve as anchoring points and provide the required chemical and biological key functions of APCs. In 2020, Wang's team reported the synthesis of a symmetrical ABA-triblock copolymer containing a middle PFPE block *via* ATRP using a difunctional PFPE macroinitiator. A series of poly(isobornyl methacrylate)-*b*-perfluoropolyether-*b*-poly(isobornyl-methacrylate) (PIBOMA-*b*-PFPE-*b*-PIBOMA) derivatives with fixed PFPE block length and different PIBOMA block lengths were synthesised and self-assembled into micelles with PIBOMA core and PFPE corona in 1,1,2-trichlorotrifluoroethane/*N,N*-dimethylformamide (F113/DMF) binary mixture. These micelles were then used to prepare hydrophobic films (water contact angle of 155° and sliding angle of 4°) by solvent evaporation at ambient temperature.¹⁵⁴

5. Perfluorocyclobutyl (PFCB)-based copolymers

The chemistry of perfluorocyclobutyl polymers (PFCB) was developed by the Dow Chemical Company in the early 1990s.¹⁵⁵ Babb pioneered the study of polymers containing 1,2-bisaryloxy-substituted perfluorocyclobutane (PFCB) ring.¹⁵⁵ PFCB ring-containing polymers with various macromolecular architectures, such as linear, branched, and cross-linked, are prepared by the [2 + 2] cycloaddition of single molecules containing multiple aryl trifluorovinyl ether groups.¹⁵⁶ Typically, thermoplastic or thermosetting PFCB polymers can be

obtained by simply heating aryl trifluorovinyl ether monomers in the bulk or in solution above 150 °C. The PFCB backbone contains equal numbers of randomly distributed *cis*- and *trans*-1,2-disubstituted hexafluorocyclobutanes. Initially developed for aerospace and microelectronics applications, PFCB polymers find use in microphotonics, coatings, nanocomposite dispersing matrix, hole transport layers for light-emitting diodes, cross-linking groups in electro-optic chromophores, and proton exchange membrane materials for hydrogen fuel cells.¹⁵⁷

Self-assemblies of amphiphilic PFCB-based copolymers were solely investigated by the group of Huang. In 2009, they reported, for the first time, the synthesis and the self-assembly behaviour of a PFCB-based block copolymer.¹⁵⁸ A new PFCB-based methacrylate monomer (TPFCBBMA) was prepared in 5 steps from 4-methylphenol (Fig. 16). Well-defined PTPFCBBMA-*b*-PEG-*b*-PTPFCBBMA amphiphilic triblock copolymers were synthesised by ATRP of TPFCBBMA from a telechelic PEG-based macroinitiator. These triblock copolymers had low solubility in water due to the significant content of hydrophobic TPFCBBMA moieties. For self-assembly, method 6 was employed. Spherical micelles were formed with a shorter hydrophobic block, while cylindrical micelles were observed when the TPFCBBMA block length was increased. However, this morphology evolution was not evidenced with TEM images.

The same group also reported the synthesis and the self-assembly of a series of well-defined semi-fluorinated amphiphilic diblock copolymers with hydrophilic PAA and fluorophilic PTPFCBBMA segments.¹⁵⁹ The PAA-*b*-PTPFCBBMA amphiphilic diblock copolymers were obtained *via* the selective acid hydrolysis of the poly(methoxymethyl acrylate) block. Method 3 was employed to trigger self-assembly. Micellar mor-

phologies were visualized by TEM. Diblock copolymers with short fluorophilic PTPFCBBMA blocks formed spherical micelles and longer PTPFCBBMA blocks led to the formation of a pearl-necklace structure. They also demonstrated that the size of the micelles could increase with increasing the length of the PTPFCBBMA block.¹⁶⁰ In 2011, the same group reported the synthesis and self-assembly of a series of well-defined semi-fluorinated amphiphilic diblock copolymers with hydrophilic PDEAEMA and fluorophilic PTPFCBBMA segments.¹⁶¹ First, RAFT homopolymerisation of TPFCBBMA was initiated by AIBN using cumyl dithiobenzoate as the chain transfer agent. Then the resulting PTPFCBBMA macro-RAFT agent was used to mediate the RAFT polymerisation of DEAEMA. Self-assembly method 6 resulted in the formation of well-ordered large spherical compound micelles (LCMs) with diameters of 400–600 nm. In 2014, they reported the synthesis of a series of well-defined ABA PBPFBCBPMA-*b*-PIB-*b*-PBPFBCBPMA triblock copolymers *via* ATRP.¹⁶² The self-assembly (using method 2) behaviour of these triblock copolymers in *n*-hexane, acetone, and 1,1,1-trifluoroacetone was investigated by TEM (Fig. 17).

The results indicated that spherical LCMs with PIB chain coronae were formed in *n*-hexane, whereas LCMs and bowl-shaped micelles with PBPFBCBPMA block coronae were produced in acetone and 1,1,1-trifluoroacetone, respectively. They also reported the preparation of “sun-shaped” amphiphilic copolymers with a PFCB aryl ether-based backbone and PAA lateral side chains.¹⁶³ The self-assembly in water of these polymers was achieved using method 6 and led to spherical micelles. In 2015, they synthesised a series of amphiphilic PFCB-based ABA triblock copolymers, PDEAEMA-*b*-PBTFVBP-*b*-PDEAEMA.¹⁶⁴ A BTFFVBP trifluorovinyl aryl ether monomer was first polymerised to form a semi-fluorinated perfluorocyclobutyl aryl ether-based segment, and end-functionalised to afford a Br-PBTFVBP-Br macroinitiator. Then, ATRP of DEAEMA was conducted in the presence of this difunctional initiator to afford PDEAEMA-*b*-PBTFVBP-*b*-PDEAEMA triblock copolymer. Self-assembly method 6 was used and spheres were formed in all processes. Since the diameters of the spheres were much larger than the calculated extended length of the triblock copolymers, the formation of LCMs was hypothesised. The authors speculated that the PBTFVBP segment formed the corona of

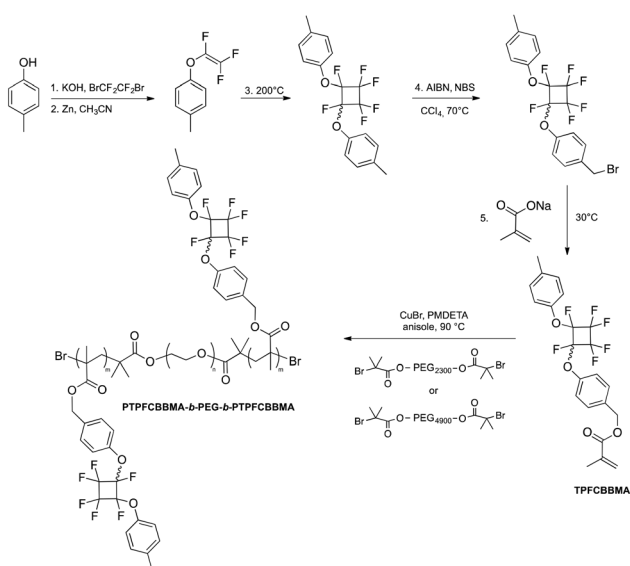


Fig. 16 Synthesis of PTPFCBBMA-*b*-PEG-*b*-PTPFCBBMA amphiphilic triblock copolymers as reported by Huang *et al.*¹⁵⁸

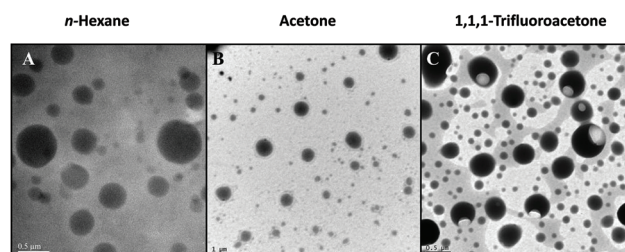


Fig. 17 TEM images of micelles formed by PBPFBCBPMA-*b*-PIB-*b*-PBPFBCBPMA triblock copolymers self-assembled in *n*-hexane (left), acetone (middle), and 1,1,1-trifluoroacetone (right). Adapted with permission from ref. 162. Copyright 2014 RSC.

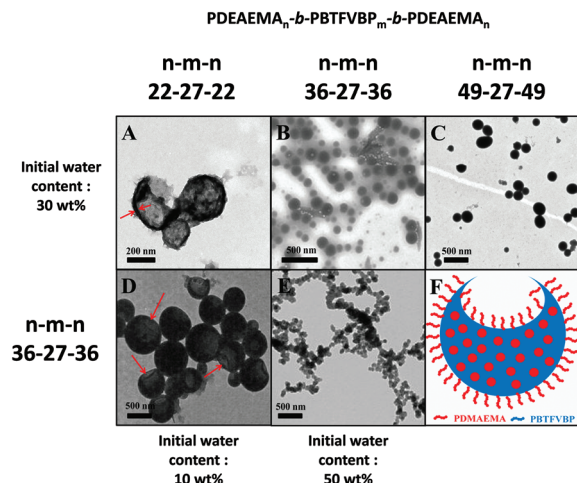
the micelles and that their core was formed from numerous reverse micelles with islands of PBTFVBP in a continuous phase of PDEAEMA. LCMs were also obtained with PDEAEMA₃₆-*b*-PBTFVBP₂₇-*b*-PDEAEMA₃₆ and PDEAEMA₄₉-*b*-PBTFVBP₂₇-*b*-PDEAEMA₄₉ containing a more extended PBTFVBP segment (diameters ranging from 100 nm to 250 nm, Fig. 18B and C). Conversely, PDEAEMA₂₂-*b*-PBTFVBP₂₇-*b*-PDEAEMA₂₂, with the lowest PDEAEMA/PBTFVBP ratio, self-assembled into vesicles of 300 nm in diameter (Fig. 18A). As the initial water content was decreased from 30 wt% to 10 wt%, bowl shaped micelles with a diameter of about 500 nm were formed for PDEAEMA₃₆-*b*-PBTFVBP₂₇-*b*-PDEAEMA₃₆ (Fig. 18D). Increasing the water content to 50 wt% resulted in 100 nm spherical micelles (Fig. 18E).

The aforementioned team synthesised amphiphilic graft copolymers bearing a hydrophobic poly(2-methyl-1,4-bis(trifluorovinyl)oxybenzene) (PMBTFVB) backbone and hydrophilic poly(ethylene glycol) (PEG) side chains.¹⁶⁵ The PMBTFVB was prepared by thermal step-growth cycloaddition polymerisation of MBTFVB and sequential end-capping with 4-methoxy-trifluorovinylbenzene. The subsequent bromination of PMBTFVB with *N*-bromosuccinimide using benzoyl peroxide as the radical initiator at 80 °C yielded PMBTFVB-Br precursors. Then, PMBTFVB-*g*-PEG copolymers were synthesised through the Williamson reaction between the hydroxyl end-group of PEG and the pendant benzyl bromide functionality of PMBTFVB-Br. Methods 3 and 5 were employed to self-assemble this graft-copolymer in water. TEM images showed diverse morphologies such as spherical micelles, spindle micelles, and large compound vesicles depending on the solvent mixture water content, copolymer concentration and preparation method. They also reported the synthesis of amphiphilic graft copolymers bearing a hydrophobic poly(2-methyl-1,4-bis(trifluorovinyl)oxybenzene) (PMBTFVB) backbone and (PAA)

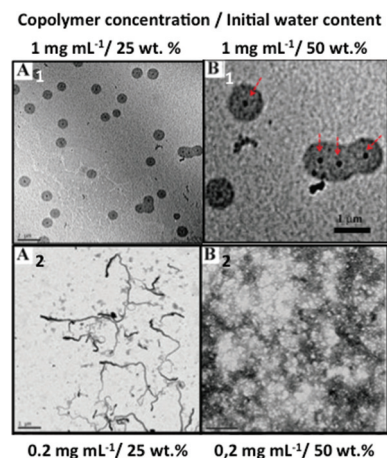
side chains.¹⁶⁶ PMBTFVB-*g*-PAA graft copolymers were synthesised by ATRP of *t*-butyl acrylate initiated by a PMBTFVB-Br macroinitiator followed by acidolysis of the hydrophobic P(*t*BA) side chains into hydrophilic PAA segments. Employing method 6, this graft-copolymer self-assembled into diverse morphologies, including vesicular, worm-like, and bowl-shaped nanostructures, depending on the water content (from 25 to 70 wt%) and the length of the PAA side chains. Vesicles (*ca.* 400–1100 nm) were formed in water:THF (25:75 wt%) binary mixture at 1 g L⁻¹ (Fig. 19A₁). The authors observed a 120 nm black dot at the centre of each vesicle that could be an artefact. A proposed explanation is that more polymer chains are found in the vesicle centre as the vesicle shells contract as a result of solvent evaporation during TEM sample preparation. In water:THF (50:50 wt%) binary mixture, 250–500 nm bowl-shaped aggregates (Fig. 19B₁) and at lower water content (25:75 wt%) micrometer-long worm-like micelles (200 nm in diameter) were obtained (Fig. 19A₂). The addition of more water before dialysis (50 wt% at 2 mg mL⁻¹) led to a network of worms (Fig. 19B₂). Decreasing the polymer concentration resulted in fewer polymer chains being able to get into the micelle structure, leading to a lower aggregation number and facilitating the morphology transformation from bilayers (vesicles) to worm-like micelles.

6. Poly(2-oxazoline)-based copolymers

Poly(oxazolines) have been studied since the 1960s, with a significant number of papers focusing on the polymerisation of 2-substituted oxazolines.^{167–170} Polymerisations are usually carried out *via* the living cationic ring-opening mechanism (CROP), producing well-defined polymers and block copolymers with narrow average molar mass distributions.^{171–174} Poly



Q12 Fig. 18 TEM images of morphologies formed from three different PDEAEMA-*b*-PBTFVBP-*b*-PDEAEMA triblock copolymers self-assembled in water when varying the initial water content. Adapted with permission from ref. 164. Copyright 2015 RSC.



Q14 Q15 Fig. 19 TEM images of the morphologies of PMBTFVB-*g*-PAA amphiphilic graft copolymers self-assembled in water when varying the initial water content and the concentration. Adapted with permission from ref. 166. Copyright 2015 RSC.

(2-oxazolines) with different properties can be prepared by varying the substituent on the monomers. In contrast to short alkyl side groups, which provide water solubility, longer analogues and aromatic side chains lead to water-insoluble polymers. Amphiphilic systems are easily accessible and can be applied, for example, as micellar catalysts, nonionic surfactants, compatibilizing agents, and for the formation of hydrogels. However, the synthesis and self-assembly behaviour of fluorinated poly(2-oxazolines)-based copolymers have been scarcely investigated.

In 2008, Papadakis *et al.*¹⁷⁵ pioneered the synthesis and self-assembly of amphiphilic fluorinated poly(2-oxazoline)-containing block copolymers in water. Amphiphilic diblock copolymers of poly(2-methyl-2-oxazoline) (PMOx) as the hydrophilic block and poly(2-(1*H*,1*H'*,2*H*,2*H'*-perfluorohexyl)-2-oxazoline) (PFOx) for the fluorophilic block were synthesised by sequential CROP. The synthesis of the PMOx-*b*-PFOx diblock copolymer was performed in an acetonitrile/chlorobenzene mixture using methyl triflate as the initiator and a three-fold excess of piperidine for termination (Fig. 20). Method 1 was employed to initiate micellization in water. As revealed by SANS and TEM, PMOx-*b*-PFOx formed elongated core/shell micelles. Schubert *et al.*¹⁷⁶ showed for the first time that well-defined gradient copolymers of 2-ethyl-2-oxazoline (EtOx) and 2-(*m*-difluorophenyl)-2-oxazoline (F2PhOx) could be prepared in one pot under microwave irradiation (Fig. 20). These gradient copolymers featured an amphiphilic character inducing the formation of self-assembled micelles in aqueous solution using method 2. Atomic force microscopy (AFM) and DLS characterization studies of the micelles indicated that the copolymers formed spherical micelles with an average diameter of around 15 nm.

In 2010, Gohy *et al.*¹⁷⁷ reported the synthesis and self-assembly of a triblock copolymer containing a fluorinated poly(2-(2,6-difluorophenyl)-2-oxazoline) (PODFOx), a lipophilic poly(2-(1-ethylheptyl)-2-oxazoline) (PEPOx), and a hydrophilic PEtOx block (Fig. 20). Aqueous solutions of this PODFOx₂₃-*b*-PEPOx₂₈-*b*-PEtOx₄₉ triblock copolymer obtained *via* method 1

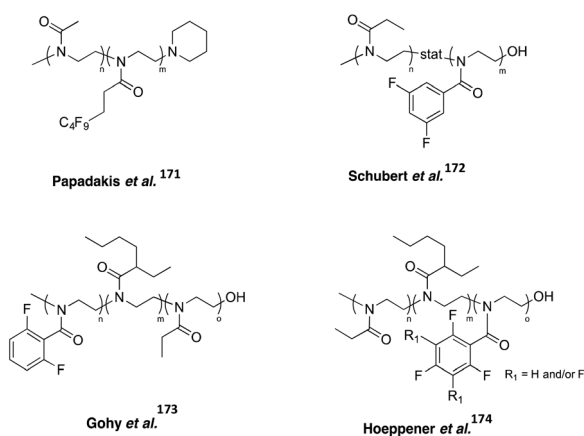


Fig. 20 Structures of self-assembled fluorinated poly(2-oxazoline)-based copolymers reported so far.

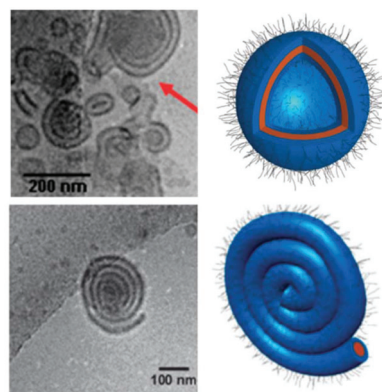


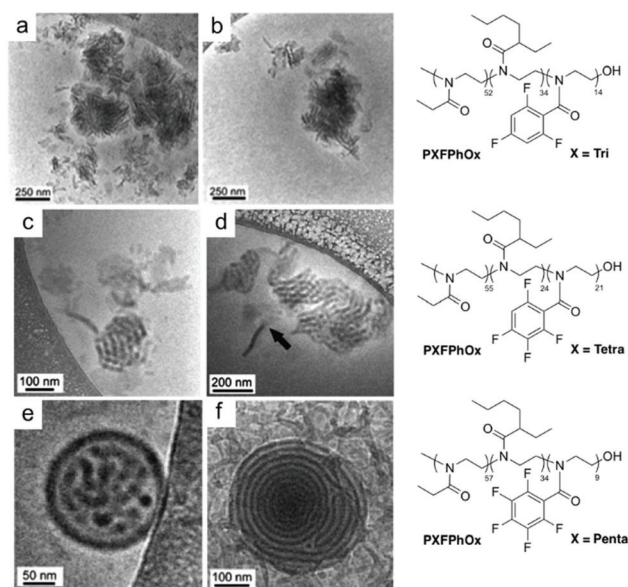
Fig. 21 Cryo-TEM pictures of micellar aggregates formed by the poly(ODFOx₂₃-*b*-EPOx₂₈-*b*-EtOx₄₉) triblock copolymer self-assembled in water. Adapted with permission from ref. 177. Copyright 2010 RSC.

showed vesicles and flat aggregates of rolled-up cylindrical micelles coexisting in water (Fig. 21).

Based on the contrast observed in the cryo-TEM images and the fact that a mixture of PODFOx and PEPOx homopolymers demixes readily, the authors hypothesised that the vesicles consisted of segregated hydrophobic domains. The rolled-up spiral aggregates were proposed to be an intermediate metastable structure between cylindrical micelles and vesicles. Supposedly, the limited solubility of the PEtOx block in water induced further aggregation of the initially formed cylindrical micelles, while the low T_g of the PEPOx block provided sufficient flexibility for the cylindrical micelles to roll-up. These two structural parameters were believed to be the key factors driving the formation of the observed rolled-up hierarchical superstructures.

Based on the promising structural features of the aforementioned work, the same authors investigated the influence of the fluorophilic character on the formation of triblock copolymer aggregates.¹⁷⁸ For this purpose, a series of PEtOx-*b*-PEPOx-*b*-PXFPPhOx (X = tri, tetra, penta) triblock copolymers were synthesised (Fig. 21). Cryo-TEM pictures revealed rod- and sheet-like morphologies for the trifluorophenyl-based triblock copolymers (Fig. 22a and b). The authors proposed a mechanism of formation based on the strong hydrophobicity of the PTriFPhOx block and the stacking of fluorinated phenyl rings caused by C–F dipole–dipole interactions. An increase of the number of fluorine atoms from PTriFPhOx to PTetraFPhOx resulted in better-defined shapes, with the presence of a few separated sheet-like structures and entangled rod-like features (Fig. 22c and d). For PPentaFPhOx blocks, well-defined supra-molecular structures were observed with perfectly round-shaped aggregates (Fig. 22e and f). Additional investigations revealed the presence of “onion-like” multilamellar vesicles with perfectly segregated concentric lamellar features. A large number of rod-like micelles were also observed alongside the well-defined complex “superaggregates”.

The ultimate thermodynamically stable structures (namely, simple and multilamellar vesicles) were prepared by tempera-



Q16 Fig. 22 Cryo-TEM pictures of micellar aggregates formed by PEtOx-*b*-PEPOx-*b*-PXPhFOx triblock copolymers self-assembled in water. Adapted with permission from ref. 178. Copyright 2013 RSC.

ture-induced equilibrium. The absence of rod-like structures led to the reasoning that the coexistence of bi-continuous and lamellar phases (non-equilibrium super aggregates) were a transition step towards the formation of more stable vesicular structures.

7. Miscellaneous

7.1. Fluorinated acrylamide

In 2013, Lee *et al.*¹⁷⁹ reported the synthesis of the thermo-responsive fluorinated polyacrylamide poly[*N*-(2,2-difluoroethyl)acrylamide]. The authors demonstrated that the thermosensitivity was easily controlled by changing the number of fluorine atoms in the terminal alkyl group of the *N*-ethyl moiety. Mono-substituted poly[*N*-(2-fluoroethyl)acrylamide] (P1F) was water-soluble, while tri-substituted poly[*N*-(2,2,2-trifluoroethyl)acrylamide] (P3F) was water-insoluble. Interestingly, di-substituted poly[*N*-(2,2-difluoroethyl)acrylamide] (P2F) exhibited a LCST around 26–28 °C in water, which was comparable to that of poly-(*N*-isopropylacrylamide) (PNIPAM). In the continuation of this work, thermo-responsive double-hydrophilic fluorinated block copolymers were synthesised by RAFT.¹⁸⁰ First, poly[*N*-(2,2-difluoroethyl)acrylamide] (P2F) was synthesised *via* RAFT polymerisation of *N*-(2,2-difluoroethyl)acrylamide (M2F) using 2-(dodecylthiocarbonylthio)-2-methylpropionic acid as the CTA. The resulting P2F macroCTA was further chain extended with *N*-(2-fluoroethyl)acrylamide (M1F) to yield poly{[*N*-(2,2-difluoroethyl)acrylamide]-*b*-[*N*-(2-fluoroethyl)acrylamide]} (P2F-*b*-P1F) diblock copolymers with different P1F lengths. Turbidimetry measured by UV-Vis spectroscopy, DLS, and *in situ* tempera-

ture-dependent ¹H NMR measurements demonstrated that the P2F block underwent a thermal transition from hydrophilic to hydrophobic, inducing the self-assembly of unimers. TEM images demonstrated that polymeric aggregates formed from an aqueous solution of P2F-*b*-P1F at 60 °C were disrupted by cooling down to 20 °C and were regenerated by heating again to 60 °C. Temperature-triggered release of a model hydrophobic drug, coumarin 102, was also demonstrated.

In 2017, Jiang *et al.*¹⁸¹ synthesised the monomer 2,2,2-trifluoroethyl 3-(*N*-(2-(diethylamino)ethyl)acrylamido)propanoate (TF-DEAE-AM) from *N,N*-diethylethylenediamine, 2,2,2-trifluoroethyl acrylate, and acryloyl chloride (Fig. 23).

TF-DEAE-AM contains both O₂⁻ and CO₂-responsive functionalities. Subsequently, a series of dual gas-responsive poly (TF-DEAE-AM) and PEG-*b*-poly(TF-DEAE-AM) were synthesised by RAFT and self-assembled in water using method 5. Due to the reaction between CO₂ and the DEAE groups, and the specific van der Waals interactions between O₂ and the trifluoromethyl groups, micelles consisting of poly(TF-DEAE-AM) or PEG-*b*-poly(TF-DEAE-AM) displayed distinct CO₂ and O₂ responsiveness in aqueous media. The authors demonstrated that pyrene (a model hydrophobic drug) could be encapsulated in the PEG-*b*-poly(TF-DEAE-AM) micelles. The release of pyrene was found to sharply increase after bubbling CO₂ or O₂ compared with N₂. Also, the highest release rate was observed in solutions treated with CO₂.

7.2. Fluorinated vinyl ether

In 1999, Yamaoka *et al.*¹⁸² reported the synthesis of fluorine-containing block copolymers consisting of poly(2-hydroxyethyl vinyl ether) (PHOVE) and poly(2-(2,2,2-trifluoroethoxy)ethyl vinyl ether) (PTFEOVE). PHOVE-*b*-PTFEOVE diblock copolymers were synthesised by living cationic polymerisation and subsequent hydrolysis. The formation of block copolymer micelles in water using method 1 was confirmed by SAXS measurements. Analysis of the SAXS profiles revealed that the micelles had a core-shell spherical morphology and the aggregation number increased when increasing the length of the PTFEOVE segment. Solubilisation experiments revealed that PHOVE-*b*-PTFEOVE BCP had a higher ability to solubilise fluorinated compounds than non-fluorinated amphiphilic BCP. The same authors confirmed this finding when they reported the synthesis and self-assembly of amphiphilic ABA (PHOVE-*b*-PFPOVE-*b*-PHOVE) (HFH), and (PFPOVE-*b*-PHOVE-*b*-PFPOVE) (FHF) (with PFPOVE corresponding to poly[2-(2,2,3,3,3-pentafluoropropoxy)ethyl vinyl ether] triblock copoly-

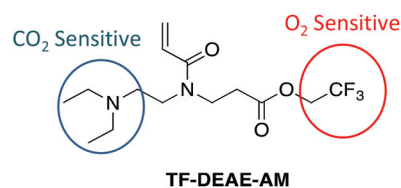


Fig. 23 Structure of TF-DEAE-AM monomer synthesised by Jiang *et al.*¹⁸¹

mers.¹⁸³ SAXS measurements revealed that HFH formed core-shell spherical micelles at a concentration of 1 wt% in aqueous solutions, whereas FHF formed more complex morphologies. In 2004, the same group reported the synthesis and self-assembly of PHOVE-*b*-PTFEOVE, PHOVE-*b*-PFPOVE, and PHOVE-*b*-HFBOVE diblock copolymers (with HFBOVE corresponding to poly[2-(2,2,3,3,4,4,4-heptafluorobutoxy)ethyl vinyl ether]).¹⁸⁴ SANS, SAXS, and DLS analyses revealed that block copolymers bearing larger fluorinated groups were more likely to form rod-like micelles without having a significant influence on the cross-sectional radii of the micelles. Scattering analysis of the copolymer micelle solutions containing hydrophobic dyes suggested that dye solubilisation strongly affected the micelle structures. The micelles became smaller as the solubility of the dye increased.

7.3. Fluorinated poly-ene

Müller *et al.*¹⁸⁵ reported the synthesis and self-assembly of fluorinated triblock copolymers derived from poly(4-*tert*-butoxystyrene)-*b*-polybutadiene-*b*-poly(*tert*-butyl methacrylate) (PtBS-*b*-PFB-*b*-PtBMA). The terpolymers were synthesised by fluorination of the PB block of PtBS-*b*-PFB-*b*-PtBMA through the radical thiol-ene reaction of the vinyl groups with 1-mercapto-1*H*,1*H*,2*H*,2*H*-perfluorooctane. These fluorinated copolymers were then self-assembled in dioxane *via* direct dissolution (method 1). Spherical micelles were formed due to microphase separation of the PtBS and PtBMA domains. Replacing dioxane with ethanol (selective solvent for PtBMA), following method 7, produced undulated bamboo-like cylindrical assemblies. Surprisingly, the cylinders were connected to each other through junctions that formed giant branched assemblies. Furthermore, the solvent-driven morphological transition between spheres and branched bamboo-like morphologies was fully reversible (Fig. 24).

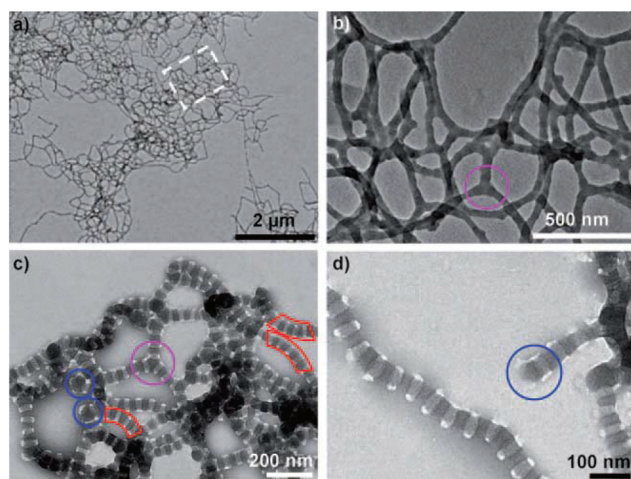


Fig. 24 (a and b) Nonstained and (c and d) RuO₄ stained TEM images of undulated cylinders obtained from ethanol dialysis of (PtBS-*b*-PFB-*b*-PtBMA) block copolymer particles in dioxane. Adapted with permission from ref. 185. Copyright 2009 Wiley.

In 2011, Mays *et al.*¹⁸⁶ reported the synthesis and self-assembly of sulfonated polystyrene-*b*-fluorinated polyisoprene (SPS-*b*-FPI) BCP. PS-*b*-FPI block copolymers were synthesised by anionic polymerisation, followed by fluorination and sulfonation. Self-assembly was achieved in water by employing method 6, and the resulting aggregates were examined by TEM. SPS-*b*-FPI with 38.8% sulfonation formed worm-like nanostructures, which changed from ribbon-shaped to tapered structures as the sample aged (one week to one month). The diblock copolymer with 29.6% sulfonation exhibited similar morphologies, although the micelles appeared to be stiffer. The authors suggested that the higher degree of sulfonation softened the assembled structure due to the increased solubility of the corona-forming chains in water.

7.4. Fluorinated polyphosphazene

In 2015, Presa-Soto *et al.*¹⁸⁷ reported the preparation of stable giant unilamellar vesicles (GUVs, diameter ≥ 1000 nm) and large vesicles (diameter ≥ 500 nm) through the self-assembly of crystalline-*b*-coil poly(di(2,2,2-trifluoroethoxy)phosphazene)-*b*-poly(methylphenylphosphazene) ($[\text{N}=\text{P}(\text{OCH}_2\text{CF}_3)_2]_n\text{-}b\text{-}[\text{N}=\text{PMePh}]_m$, PTFEP-*b*-PMPP, $n = 30/m = 20$, $n = 90/m = 20$, or $n = 200/m = 85$) diblock copolymers in THF. This block copolymer combined crystalline but flexible PTFEP and amorphous PMPP blocks. SEM, TEM, and WAXS experiments demonstrated that the stability of these GUVs was caused by the crystallization of PTFEP blocks in the walls of the GUVs. Higher degrees of crystallinity of the GUV walls were observed in the larger vesicles. This suggested that the crystallinity of the PTFEP block facilitated the formation of large vesicles. The GUVs were responsive to strong acids and, after selective protonation of the PMPP block, they underwent a morphological transition to smaller spherical micelles within which the core and corona were inverted. This morphological evolution was completely reversible upon neutralization with a base, regenerating the original GUVs (Fig. 25).

The same group also showed that bicontinuous nanospheres or toroidal micelles could be produced by the self-assembly of a single crystalline-*b*-coil (PTFEP-*b*-PS) diblock

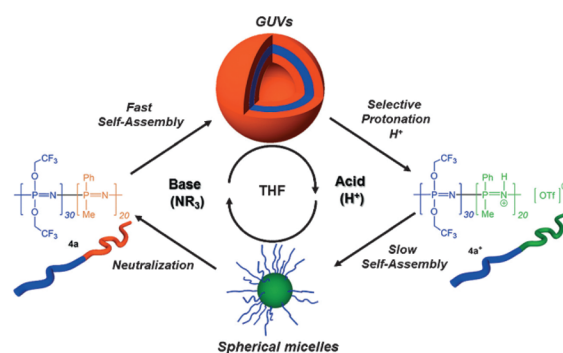


Fig. 25 Schematic representation of the reversible morphological evolution from GUVs to spherical vesicles promoted by a selective acid-base reaction. Reproduced with permission from ref. 187. Copyright 2015 Wiley.

1 copolymer in THF (without additives), by simply adjusting the
 2 **Q19** block copolymer concentration.¹⁸⁸ Moreover, these two rare
 3 morphologies were reversibly interchanged in THF, by simple
 4 dilution (adding THF) or concentration (evaporating THF) of
 5 the block copolymer solution. The crystallinity of the core-
 6 forming PTFEP block appeared to be the main driving force
 7 for the formation of bicontinuous nanospheres and toroidal
 8 micelles. Hence, the self-assembly of a linear PTFEP-*b*-PS
 9 diblock copolymer to form bicontinuous or toroidal micelles
 10 can be controlled by modulating the crystallization of the
 11 PTFEP segments by simply changing the block copolymer
 12 concentration.

7.5. Fluorinated siloxane

15 In 2012, Perahia *et al.*¹⁸⁹ reported the self-assembly of a poly
 16 (semi-fluorinated siloxane)-containing diblock copolymer, poly
 17 (3,3,3-trifluoropropyl methylsiloxane)-*b*-polystyrene (PSiF-*b*-PS),
 18 in toluene (a selective solvent for PS). The high incompatibility
 19 of the PSiF block drove aggregation. For example, the sym-
 20 metric triblock copolymer formed elliptical micelles with
 21 unique temperature stability, compared with aggregates
 22 formed from diblock copolymers in the lower segregation
 23 regime. The micelles had a relatively low aggregation number
 24 and contained high amounts of solvent in their core. As
 25 expected, the curvature of the core–corona interface was sig-
 26 nificantly affected by the volume fraction of the PSiF block.

27 In 2015, Manners *et al.*¹⁹⁰ investigated the self-assembly of
 28 diblock copolymers containing a crystalline poly(ferrocenyldi-
 29 methylsilane) (PFS) block and a poly(fluorinated siloxane) coil
 30 block (PFMVS = poly(methylvinylsiloxane) with 1*H*,1*H*,2*H*,2*H*-
 31 perfluorooctane dangling chains). Direct dissolution (method
 32 1) of the block copolymer in trifluorotoluene (TFT) did not
 33 result in the formation of any aggregates, even after 24 h.
 34 However, when the polymer solution was allowed to stand for
 35 one week, cylindrical micelles with PFS cores were formed
 36 (Fig. 26).

37 Self-seeding protocols were also successfully employed to
 38 prepare micelles with controlled lengths and structures and
 39 low polydispersities. Finally, partial functionalisation of the
 40 PFMVS block copolymers with a fluorescent dye led to the for-
 41 mation of well-defined, functional nanomaterials.

42 In 2015, Dong *et al.*¹⁹¹ reported the solution self-assembly
 43 of an ABC block terpolymer consisting of a polystyrene-*b*-poly
 44 (ethylene oxide) (PS-*b*-PEO) diblock copolymer tail tethered to
 45 a fluorinated polyhedral oligomeric silsesquioxane (FPOSS)
 46 cage. This terpolymer was self-assembled in 1,4-dioxane/water
 47 binary mixture using method 2. At a low water content
 48 (10 wt%), spherical micelles with uniform size distributions
 49 were produced. A sphere to worm transition was observed
 50 when the water content increased to 18 wt%. Other circular
 51 morphologies were formed at water contents ranging from 22
 52 to 34 wt%, including toroids (Fig. 27a), tadpoles and dumb-
 53 bells (Fig. 27b), interlocked toroids (Fig. 27c), *etc.* Toroid was
 54 the prevalent morphology. These toroidal structures had
 55 similar diameters and an identical core–shell–corona molecu-
 56 lar arrangement to that of the worm-like micelles. For this

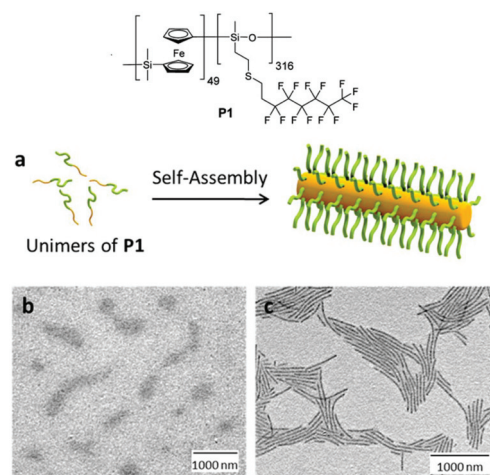


Fig. 26 Schematic representation of the self-assembly of PFS-*b*-PFMVS leading to cylindrical micelles. PFS = yellow, PFMVS functionalised with perfluoroalkane = light green (a). TEM micrographs of a drop-cast sample in TFT (60 mg mL⁻¹) after 24 h (b) and 1 week (c). Reproduced with permission from ref. 190. Copyright 2015 ACS.

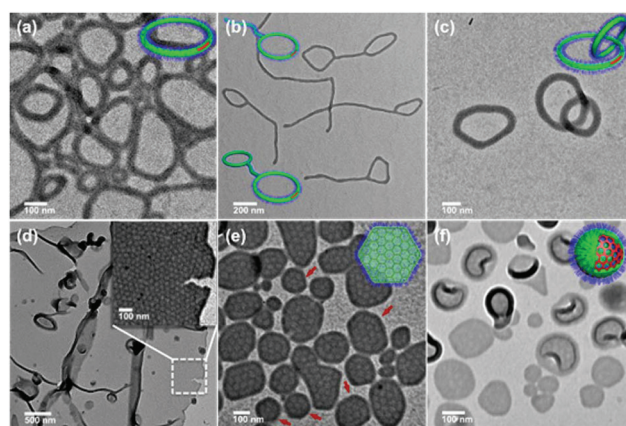


Fig. 27 TEM images of (a) toroids, (b) tadpoles and dumbbells, (c) interlocked toroids, (d and e) 2D nanosheets, and (f) laterally structured vesicles. FPOSS = red; PS = green; PEO = blue. Reproduced with permission from ref. 191. Copyright 2015 ACS.

45 reason, they were supposed to arise from the closure of worm-
 46 like micelles due to the increasing water content (Fig. 27).
 47 Lateral aggregation and fusion of the worm-like micelles also
 48 resulted in primitive nano-sheets stabilised by thicker rims to
 49 partially release the rim-cap energy. Rearrangement of the par-
 50 allel-aligned FPOSS cylindrical cores generated hexagonally
 51 patterned nanosheets.

7.6. Poly(vinylidene fluoride)-based copolymers (PVDF)

52 In 2010, Gohy *et al.*¹⁹² reported the self-assembly of the blend
 53 poly(VDF-*ter*-HFP-*ter*-MAF) terpolymer and PS-*b*-P2VP-*b*-PEO
 54 triblock terpolymer (VDF = vinylidene fluoride, HFP = hexa-
 55 fluoropropene). The micellar solutions were obtained by first
 56 dissolving one of the blend partners in DMF, followed by the

addition of the second blend partner as a powder. The formation of hydrogen-bonded complexes between MAF and P2VP units was observed, leading to insoluble micelles of P2VP/poly(VDF-*ter*-HFP-*ter*-TFMA) terpolymer cores surrounded by a mixture of PS and PEO chains. Later, Asandei *et al.*¹⁹³ reported the self-assembly of PNaSS-*b*-PVDF-*b*-PNaSS triblock copolymers synthesised by deprotection of the neopentyl styrene sulfonate (NpSS) groups in PNpSS-*b*-PVDF-*b*-PNpSS triblock copolymers with NaN₃. Using methods 1 and 3, all PNaSS-*b*-PVDF-*b*-PNaSS triblock copolymers provided colloidal stable nanoparticles in aqueous solution, even under the relatively high ionic strength of phosphate buffered saline (PBS) solutions (pH = 7.4, 0.01 M phosphate buffer, 0.0027 M potassium chloride and 0.137 M sodium chloride). Ladmiral and co-workers reported the preparation and aqueous self-assembly of PVDF-*b*-PVA diblock copolymers obtained by RAFT polymerisation followed by basic hydrolysis (PVA = poly(vinyl alcohol)).¹⁹⁴ Using method 7, spherical nanoobjects with PVDF cores and PVA shells with diameters of about 147 nm were observed. Protocols of VDF RAFT dispersion polymerisation in the presence of PVAc macro-CTAs were also published (PVAc = poly(vinyl acetate)).¹⁹⁵ These PISA protocols afforded PVAc-*b*-PVDF branched micrometer-long crystalline morphologies resembling a desert rose (Fig. 28). Although self-assembly was triggered by the PVDF growing block, the morphologies of these structures were thought to be governed by the crystallization of PVDF. The crystallization-driven self-assembly (CDSA) approach was also employed by the same authors with amphiphilic PVDF-*b*-PDMAEMA block copolymers.¹⁹⁶ These BCPs were synthesised by CuAAC click chemistry of an azide-functionalised PVDF prepared by RAFT polymerisation and three alkyne-functionalised PDMAEMAs prepared by ATRP. The three well-defined PVDF-*b*-PDMAEMA block copolymers were then self-assembled in water at three different pH values. Mainly ill-defined spherical particles in the 20 to 500 nm size range were observed. However, micrometer-long cylindrical rigid micelles were obtained for PDMAEMA with DP = 63 at pH 8.

The same group also synthesised ABA triblock copolymers containing PVDF segments. Using a “one-pot” approach they prepared PVDF-*b*-PEG-*b*-PVDF and P(VDF-*co*-HFP)-*b*-PEG-*b*-P(VDF-*co*-HFP) *via* efficient thia-Michael addition coupling of PVDF or P(VDF-HFP) prepared by RAFT, and a PEG

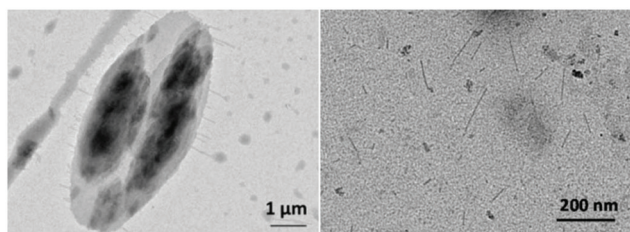


Fig. 28 Desert rose-like morphologies synthesised through PISA (PVAc-*b*-PVDF BCs, left) and cylindrical rigid micelles (PVDF-*b*-PDMAEMA BCs, right) reported by Ladmiral *et al.*^{195,196} Copyright 2017 RSC.

diacrylate.^{197,198} These symmetrical triblock copolymers led to various morphologies, depending on the solvent mixtures and the self-assembly method. For example, PVDF-*b*-PEG-*b*-PVDF in THF/H₂O mixtures always formed vesicles, regardless of the solvent ratios or self-assembly method. In contrast, when THF/ethanol mixtures (1:4 and 1:6) and method 2 were used, ovoidal shapes and crystalline shards were observed. These self-assemblies are believed to be governed by the high crystallinity of the PVDF block. Incorporation of HFP into the fluorinated blocks of the ABA triblock copolymer reduced the crystallinity and allowed easier access to and control over the formation of uncommon crystalline structures.¹⁹⁸ In another study, Ladmiral *et al.* reported the synthesis and self-assembly of poly(*N*-isopropylacrylamide)-*b*-PVDF and PNIPAM-*b*-PVDF amphiphilic block copolymers using RAFT polymerisation. A PNIPAM macro-CTA was used to polymerise VDF in dimethyl carbonate (DMC). The as prepared diblock copolymers were self-assembled in various solvent mixtures using the solvent CDSA method (method 2). Some of the outstanding morphologies observed were crumpled spheres (PNIPAM₂₅-*b*-PVDF₃₅ and PNIPAM₃₅-*b*-PVDF₄₅₀ in DMF : water (1 : 4)), bilayer aggregates (PNIPAM₃₅-*b*-PVDF₄₅₀ in THF : water (1 : 4)), and 2D lenticular micelles (PNIPAM₂₅-*b*-PVDF₃₅ in acetone : water (1 : 4)).¹⁹⁹ Qian *et al.*²⁰⁰ reported the self-assembly of commercially available PVDF-*b*-PS block copolymers. Micelle preparations were achieved *via* method 1 in different solvent mixtures and using two different block copolymers (PVDF₁₈₀-*b*-PS₁₂₅ and PVDF₁₈₀-*b*-PS₁₂₀₂). Irregular spherical micelles were obtained, except for PVDF₁₈₀-*b*-PS₁₂₅, which led to worm-like micelles in DMF : 1,4-dioxane (80 : 20).

7.7. Poly(ionic liquid)

Fluorinated poly(ionic liquid)s (PILs) have also attracted interest, either to promote morphology transitions when the fluorinated moieties were introduced as counter ions (*e.g.* the most used bis(trifluoromethylsulfonyl)imide(TFSI⁻)), or as a constituent of the backbone to induce self-organization. For instance, Vijayakrishna *et al.* reported a sudden yet fully reversible modification of PIL BCP microstructures using anion exchange.²⁰¹ When bromide counter ions were exchanged with TFSI⁻, a reversible transition from micelles to vesicles was observed. A similar morphological transition (sphere to vesicle) was also observed with imidazolium poly(ionic liquid) when silver hexafluoroborate salt was employed.²⁰² This microstructure evolution triggered by counter ion exchange was later confirmed by Isik *et al.* They extended this concept to 4 different polyelectrolytes of different molar masses.²⁰³ They demonstrated that the size of the nanoparticles could be tuned in the range of 100–600 nm, depending on the chemical structure, molar mass and relative amount of TFSI⁻ added *vs.* the initial halide. He *et al.* reported the self-assembly of poly(acrylic acid)-*b*-poly(4-vinylbenzyl)-3-butyl imidazolium (TFSI⁻) block copolymer into micelles, lamellae and cubosomes.²⁰⁴ The morphologies were obtained in THF/H₂O mixtures using method 2 without removing the good solvent (THF) from the mixture. The cubosomes were particularly interesting, consid-

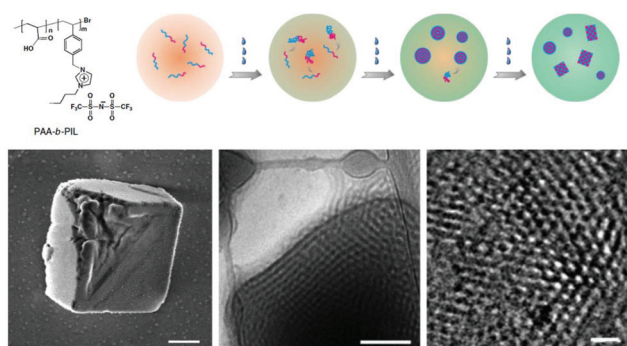


Fig. 29 (Top) BC structure and proposed self-assembly process of PAA-*b*-PIL in THF/H₂O with the addition of water, resulting in the formation of cubosomes. (Bottom) SEM micrograph of the dried cubosomes after dialysis. (b) Cryo-TEM image of the [100] facet of a cuboid particle. (c) Enlarged surface image recorded in the central area of a cuboid particle from the [111] facet. Adapted with permission from ref. 204. Copyright Springer Nature 2016.

ering their unique characteristics in the context of BCP self-assembly (Fig. 29).²⁰⁵

However, the formation of these nanostructures was only observed under very specific conditions with a complex self-assembling pathway, suggesting that ionic interactions could be one of the major governing parameters. Many other PIL BCP microstructures were also reported with fluorinated counter ions, such as TFSI⁻, PF₆⁻, BF₄⁻, and OTf⁻ (CF₃SO₃⁻), although the fluorinated contribution was not always the prevailing factor in self-assembly.^{206–208}

Lately, a novel fluorinated-PIL featuring C₆F₁₃ pendent groups, as a structuring agent able to promote self-assembly and ensure good thermal, mechanical and conductive properties, was reported. In this study, BCP synthesis was achieved *via* an elegant strategy involving a one-pot process using cobalt-mediated radical polymerisation-induced self-assembly (CMR-PISA).²⁰⁹

8. Conclusion

Given the numerous potential applications of fluorinated copolymers, there is constantly growing interest in developing new methodologies to prepare them. Aside from coupling chemistries, recent advances in reversible deactivation radical polymerisation (RDRP) have opened new possibilities to prepare such copolymers. The aim of this review article was to gather a concise record of the methods used to prepare fluorinated amphiphilic copolymers that led to self-assemblies in solution. Indeed, solution self-assembly is an attractive way to obtain colloidal stable nano-structures if it can be controlled and reproduced with high reliability. Given the wealth of properties that can be brought by fluorinated polymer blocks (low *T_g*, crystallinity, O₂-philicity, hydrophobicity, oleophobicity, or ferroelectricity to name a few) fluorinated copolymer-based nano-objects should find applications in future nano-technologies.

Conflicts of interest

Authors declare no conflict of interest.

Acknowledgements

The authors thank Professor D. Taton for his precious advice and co-workers cited in the references below.

Notes and references

- S. C. Glotzer and M. J. Solomon, *Nat. Mater.*, 2007, **6**, 557–562.
- J. Yan, M. Bloom, S. C. Bae, E. Luijten and S. Granick, *Nature*, 2012, **491**, 578–581.
- A. H. Gröschel, A. Walther, T. I. Löbbling, F. H. Schacher, H. Schmalz and A. H. E. Müller, *Nature*, 2013, **503**, 247–251.
- L. Cademartiri and K. J. M. Bishop, *Nat. Mater.*, 2015, **14**, 2–9.
- Z. Hua, J. R. Jones, M. Thomas, M. C. Arno, A. Souslov, T. R. Wilks and R. K. O'Reilly, *Nat. Commun.*, 2019, **10**, 1–8.
- L. Zhang and A. Eisenberg, *Science*, 1995, **268**, 1728–1731.
- L. Zhang and A. Eisenberg, *J. Am. Chem. Soc.*, 1996, **118**, 3168–3181.
- D. E. Discher and A. Eisenberg, *Science*, 2002, **297**, 967–973.
- U. Tritschler, S. Pearce, J. Gwyther, G. R. Whittell and I. Manners, *Macromolecules*, 2017, **50**, 3439–3463.
- Y. Mai and A. Eisenberg, *Chem. Soc. Rev.*, 2012, **41**, 5969–5985.
- J. Rodríguez-Hernández, F. Chécot, Y. Gnanou and S. Lecommandoux, *Prog. Polym. Sci.*, 2005, **30**, 691–724.
- H. Qiu, Z. M. Hudson, M. A. Winnik and I. Manners, *Science*, 2015, **347**, 1329–1332.
- J. Schmelz, F. H. Schacher and H. Schmalz, *Soft Matter*, 2013, **9**, 2101–2107.
- N. Houbenov, R. Milani, M. Poutanen, J. Haataja, V. Dichiarante, J. Sainio, J. Ruokolainen, G. Resnati, P. Metrangolo and O. Ikkala, *Nat. Commun.*, 2014, **5**, 1–8.
- L. Meazza, J. A. Foster, K. Fucke, P. Metrangolo, G. Resnati and J. W. Steed, *Nat. Chem.*, 2013, **5**, 42–47.
- H. Cui, Z. Chen, S. Zhong, K. L. Wooley and D. J. Pochan, *Science*, 2007, **317**, 647–650.
- Y. Yan, J. Huang and B. Z. Tang, *Chem. Commun.*, 2016, **52**, 11870–11884.
- M. A. Hillmyer and T. P. Lodge, *J. Polym. Sci., Part A: Polym. Chem.*, 2002, **40**, 1–8.
- C. K. Wong, X. Qiang, A. H. E. Müller and A. H. Gröschel, *Prog. Polym. Sci.*, 2020, 101211.
- A. O. Moughton, M. A. Hillmyer and T. P. Lodge, *Macromolecules*, 2012, **45**, 2–19.
- J. Huang, Y. Guo, S. Gu, G. Han, W. Duan, C. Gao and W. Zhang, *Polym. Chem.*, 2019, **10**, 3426–3435.

- 1 22 W. Yao, Y. Li and X. Huang, *Polymer*, 2014, **55**, 6197–6211.
- 23 J. Gardiner, *Aust. J. Chem.*, 2015, **68**, 13.
- 24 T. P. Lodge, A. Rasdal, Z. Li and M. A. Hillmyer, *J. Am. Chem. Soc.*, 2005, **127**, 17608–17609.
- 5 25 A. H. Gröschel, F. H. Schacher, H. Schmalz, O. V. Borisov, E. B. Zhulina, A. Walther and A. H. E. Müller, *Nat. Commun.*, 2012, **3**, 710.
- 26 Y. Zhao, F. Sakai, L. Su, Y. Liu, K. Wei, G. Chen and M. Jiang, *Adv. Mater.*, 2013, **25**, 5215–5256.
- 10 27 L. He, J. P. Hinestrosa, J. M. Pickel, S. Zhang, D. G. Bucknall, S. M. K. Ii, J. W. Mays and K. Hong, *J. Polym. Sci., Part A: Polym. Chem.*, 2011, **49**, 414–422.
- 15 28 H. Peng, K. J. Thurecht, I. Blakey, E. Taran and A. K. Whittaker, *Macromolecules*, 2012, **45**, 8681–8690.
- 29 K. Wang, H. Peng, K. J. Thurecht, S. Puttick and A. K. Whittaker, *Polym. Chem.*, 2016, **7**, 1059–1069.
- 30 30 G. Li, A. Xu, B. Geng, S. Yang, G. Wu and S. Zhang, *J. Fluor. Chem.*, 2014, **165**, 132–137.
- 31 P. I. R. Muraro, A. G. O. de Freitas, S. G. Trindade, F. C. Giacomelli, J.-J. Bonvent, V. Schmidt, F. P. dos Santos and C. Giacomelli, *J. Fluor. Chem.*, 2014, **168**, 251–259.
- 32 Q. Zhang and S. Zhu, *ACS Macro Lett.*, 2014, **3**, 743–746.
- 25 33 Y. Chen, Y. Zhang, Y. Wang, C. Sun and C. Zhang, *J. Appl. Polym. Sci.*, 2013, **127**, 1485–1492.
- 34 Y. Xu, W. Wang, Y. Wang, J. Zhu, D. Uhrig, X. Lu, J. K. Keum, J. W. Mays and K. Hong, *Polym. Chem.*, 2016, **7**, 680–688.
- 30 35 W. Du, A. M. Nyström, L. Zhang, K. T. Powell, Y. Li, C. Cheng, S. A. Wickline and K. L. Wooley, *Biomacromolecules*, 2008, **9**, 2826–2833.
- 36 K. Y. Mya, E. M. J. Lin, C. S. Gudipati, H. B. A. S. Gose and C. He, *J. Phys. Chem. B*, 2010, **114**, 9128–9134.
- 35 **Q22** 37 H. Liu, Y. Zhao, C. A. Dreiss and Y. Feng, *Soft Matter*, 2014, **10**, 6387–6391.
- 38 H. Liu, W. Wang, H. Yin and Y. Feng, *Langmuir*, 2015, **31**, 8756–8763.
- 40 39 H. Liu, Z. Guo, S. He, H. Yin and Y. Feng, *RSC Adv.*, 2016, **6**, 86728–86735.
- 40 40 S.-D. Xiong, L. Li, S.-L. Wu, Z.-S. Xu and P. K. Chu, *J. Polym. Sci., Part A: Polym. Chem.*, 2009, **47**, 4895–4907.
- 41 B. Jiang and H. Pang, *J. Polym. Sci., Part A: Polym. Chem.*, 2016, **54**, 992–1002.
- 45 42 J.-N. Marsat, M. Heydenreich, E. Kleinpeter, H. V. Berlepsch, C. Böttcher and A. Laschewsky, *Macromolecules*, 2011, **44**, 2092–2105.
- 43 Y.-N. Zhou, H. Cheng and Z.-H. Luo, *J. Polym. Sci., Part A: Polym. Chem.*, 2011, **49**, 3647–3657.
- 50 44 B. P. Koiry, A. Chakrabarty and N. K. Singha, *RSC Adv.*, 2015, **5**, 15461–15468.
- 45 B. P. Koiry, S. Ponnupandian, S. Choudhury and N. K. Singha, *J. Fluor. Chem.*, 2016, **189**, 51–58.
- 55 46 L. Yu, J.-J. Qiu, H. Cheng and Z.-H. Luo, *Mater. Chem. Phys.*, 2013, **138**, 780–786.
- 47 J. Chen, J.-J. Li and Z.-H. Luo, *J. Polym. Sci., Part A: Polym. Chem.*, 2013, **51**, 1107–1117.
- 48 M. V. de Paz Bález, K. L. Robinson, V. Bütün and S. P. Armes, *Polymer*, 2001, **42**, 29–37.
- 49 J. Mao, P. Ni, Y. Mai and D. Yan, *Langmuir*, 2007, **23**, 5127–5134.
- 50 J. He, P. Ni and C. Liu, *J. Polym. Sci., Part A: Polym. Chem.*, 2008, **46**, 3029–3041.
- 51 Y. Hao, M. Zhang, J. Xu, C. Liu and P. Ni, *J. Macromol. Sci., Part A: Pure Appl. Chem.*, 2010, **47**, 941–951.
- 52 S. Li, J. He, M. Zhang, H. Wang and P. Ni, *Polym. Chem.*, 2016, **7**, 1773–1781.
- 10 53 X. Liu, Y. Ding, J. Liu, S. Lin and Q. Zhuang, *Eur. Polym. J.*, 2019, **116**, 342–351.
- 54 J. Liu, Y. Ding, X. Liu, S. Lin and Q. Zhuang, *Eur. Polym. J.*, 2019, **118**, 465–473.
- 15 55 S. Houvenagel, L. Moine, G. Picheth, C. Dejean, A. Brûlet, A. Chennevière, V. Faugeras, N. Huang, O. Couture and N. Tsapis, *Biomacromolecules*, 2018, **19**, 3244–3256.
- 56 K. Matsumoto, T. Ishizuka, T. Harada and H. Matsuoka, *Langmuir*, 2004, **20**, 7270–7282.
- 20 57 W. Wang, J. Zhang, C. Li, P. Huang, S. Gao, S. Han, A. Dong and D. Kong, *Colloids Surf., B*, 2014, **115**, 302–309.
- 58 H. Hussain, K. Busse and J. Kressler, *Macromol. Chem. Phys.*, 2003, **204**, 936–946.
- 25 59 H. S. Hwang, H. J. Kim, Y. T. Jeong, Y.-S. Gal and K. T. Lim, *Macromolecules*, 2004, **37**, 9821–9825.
- 60 Y. Koda, T. Terashima and M. Sawamoto, *Macromolecules*, 2016, **49**, 4534–4543.
- 30 61 J. H. Ko, A. Bhattacharya, T. Terashima, M. Sawamoto and H. D. Maynard, *J. Polym. Sci., Part A: Polym. Chem.*, 2019, **57**, 352–359.
- 62 M. Matsumoto, M. Sawamoto and T. Terashima, *ACS Macro Lett.*, 2019, **8**, 320–325.
- 35 63 M. Y. Lee, S. H. Kim, J. T. Kim, S. W. Kim and K. T. Lim, *J. Nanosci. Nanotechnol.*, 2008, **8**, 4864–4868.
- 64 S. Xu and W. Liu, *J. Polym. Sci., Part B: Polym. Phys.*, 2008, **46**, 1000–1006.
- 40 65 X. Dong, L. He, N. Wang, J.-Y. Liang, M.-J. Niu and X. Zhao, *J. Mater. Chem.*, 2012, **22**, 23078–23090.
- 66 Y. Zhang, L. Wang, Z. Zhang, Y. Zhang and X. Tuo, *J. Polym. Sci., Part A: Polym. Chem.*, 2013, **51**, 2161–2170.
- 67 A. Pan, S. Yang and L. He, *RSC Adv.*, 2015, **5**, 55048–55058.
- 45 68 X. Ma, L. He, S. Huang, Y. Wu, A. Pan and J. Liang, *Colloid Polym. Sci.*, 2020, **298**, 1559–1569.
- 69 T. Imae, H. Tabuchi, K. Funayama, A. Sato, T. Nakamura and N. Amaya, *Colloids Surf., A*, 2000, **167**, 73–81.
- 70 K. Skrabania, A. Laschewsky, H. V. Berlepsch and C. Böttcher, *Langmuir*, 2009, **25**, 7594–7601.
- 50 71 H. V. Berlepsch, C. Böttcher, K. Skrabania and A. Laschewsky, *Chem. Commun.*, 2009, 2290–2292.
- 72 K. Skrabania, H. V. Berlepsch, C. Böttcher and A. Laschewsky, *Macromolecules*, 2010, **43**, 271–281.
- 55 73 Y. Gao, X. Li, L. Hong and G. Liu, *Macromolecules*, 2012, **45**, 1321–1330.
- 74 X. Li, Y. Gao, X. Xing and G. Liu, *Macromolecules*, 2013, **46**, 7436–7442.

- 1 75 X. Li, B. Jin, Y. Gao, D. W. Hayward, M. A. Winnik, Y. Luo and I. Manners, *Angew. Chem., Int. Ed.*, 2016, **55**, 11392–11396.
- 5 76 B. Jin, K. Sano, S. Aya, Y. Ishida, N. Gianneschi, Y. Luo and X. Li, *Nat. Commun.*, 2019, **10**, 1–8.
- 77 X. Li, Y. Yang, G. Li and S. Lin, *Polym. Chem.*, 2014, **5**, 4553–4560.
- 78 G. Cavallo, P. Metrangolo, R. Milani, T. Pilati, A. Priimagi, G. Resnati and G. Terraneo, *Chem. Rev.*, 2016, **116**, 2478–2601.
- 10 79 A. Vanderkooy and M. S. Taylor, *J. Am. Chem. Soc.*, 2015, **137**, 5080–5086.
- 80 S. Banerjee, V. Ladmiral, A. Debuigne, C. Detrembleur, S. M. W. Rahaman, R. Poli and B. Ameduri, *Macromol. Rapid Commun.*, 2017, **38**, 1700203.
- 15 81 S. Banerjee, E. V. Bellan, F. Gayet, A. Debuigne, C. Detrembleur, R. Poli, B. Améduri and V. Ladmiral, *Polymers*, 2017, **9**, 702.
- 20 82 S. Banerjee, V. Ladmiral, C. Totée and B. Améduri, *Eur. Polym. J.*, 2018, **104**, 164–169.
- 83 P. G. Falireas, V. Ladmiral and B. Ameduri, *Polym. Chem.*, 2021, **12**, 277–290.
- 25 84 H. S. Hwang, J. Y. Heo, Y. T. Jeong, S.-H. Jin, D. Cho, T. Chang and K. T. Lim, *Polymer*, 2003, **44**, 5153–5158.
- 85 M. Niu, L. He, J. Liang, A. Pan and X. Zhao, *Prog. Org. Coat.*, 2014, **77**, 1603–1612.
- 30 86 C. Mugemana, B.-T. Chen, K. V. Bukhryakov and V. Rodionov, *Chem. Commun.*, 2014, **50**, 7862–7865.
- 87 B. Charleux, G. Delaittre, J. Rieger and F. D'Agosto, *Macromolecules*, 2012, **45**, 6753–6765.
- 88 S. L. Canning, G. N. Smith and S. P. Armes, *Macromolecules*, 2016, **49**, 1985–2001.
- 35 89 N. J. W. Penfold, J. Yeow, C. Boyer and S. P. Armes, *ACS Macro Lett.*, 2019, **8**, 1029–1054.
- 90 C. Liu, C.-Y. Hong and C.-Y. Pan, *Polym. Chem.*, 2020, **11**, 3673–3689.
- 40 91 F. D'Agosto, J. Rieger and M. Lansalot, *Angew. Chem., Int. Ed.*, 2020, **59**, 8368–8392.
- 92 A. B. Lowe, *Polymer*, 2016, **106**, 161–181.
- 93 X. Wang and Z. An, *Macromol. Rapid Commun.*, 2019, **40**, 1800325.
- 45 94 N. J. W. Penfold, J. Yeow, C. Boyer and S. P. Armes, *ACS Macro Lett.*, 2019, **8**, 1029–1054.
- 95 S. Li, G. Han and W. Zhang, *Polym. Chem.*, 2020, **11**, 4681–4692.
- 96 S. R. Mane, *New J. Chem.*, 2020, **44**, 6690–6698.
- 50 97 J. Rieger, *Macromol. Rapid Commun.*, 2015, **36**, 1458–1471.
- 98 M. Zong, K. J. Thurecht and S. M. Howdle, *Chem. Commun.*, 2008, 5942–5944.
- 99 A. Xu, Q. Lu, Z. Huo, J. Ma, B. Geng, U. Azhar, L. Zhang and S. Zhang, *RSC Adv.*, 2017, **7**, 51612–51620.
- 55 100 M. Semsarilar, E. R. Jones and S. P. Armes, *Polym. Chem.*, 2013, **5**, 195–203.
- 101 M. Semsarilar, V. Ladmiral, A. Blanazs and S. P. Armes, *Polym. Chem.*, 2014, **5**, 3466–3475.
- 102 B. Akpınar, L. A. Fielding, V. J. Cunningham, Y. Ning, O. O. Mykhaylyk, P. W. Fowler and S. P. Armes, *Macromolecules*, 2016, **49**, 5160–5171.
- 103 G. N. Smith, M. J. Derry, J. E. Hallett, J. R. Lovett, O. O. Mykhaylyk, T. J. Neal, S. Prévost and S. P. Armes, *Proc. R. Soc. A*, 2019, **475**, 20180763.
- 104 J. Jennings, E. J. Cornel, M. J. Derry, D. L. Beattie, M. J. Rymaruk, O. J. Deane, A. J. Ryan and S. P. Armes, *Angew. Chem., Int. Ed.*, 2020, **59**, 10848–10853.
- 10 105 L. Guo, Y. Jiang, T. Qiu, Y. Meng and X. Li, *Polymer*, 2014, **55**, 4601–4610.
- 106 W. Zhao, H. T. Ta, C. Zhang and A. K. Whittaker, *Biomacromolecules*, 2017, **18**, 1145–1156.
- 107 F. Ouhib, A. Dirani, A. Aqil, K. Glinel, B. Nysten, A. M. Jonas, C. Jérôme and C. Detrembleur, *Polym. Chem.*, 2016, **7**, 3998–4003.
- 15 108 X. Chen, J. Zhou and J. Ma, *RSC Adv.*, 2015, **5**, 97231–97238.
- 109 J. Zhou, X. Chen and J. Ma, *Prog. Org. Coat.*, 2016, **100**, 86–93.
- 20 110 J. Zhou, R. He and J. Ma, *Polymers*, 2016, **8**, 207.
- 111 J. Zhou, R. He and J. Ma, *Polymers*, 2016, **8**, 384.
- 112 M. Huo, M. Zeng, D. Li, L. Liu, Y. Wei and J. Yuan, *Macromolecules*, 2017, **50**, 8212–8220.
- 25 113 M. Huo, D. Li, G. Song, J. Zhang, D. Wu, Y. Wei and J. Yuan, *Macromol. Rapid Commun.*, 2018, **39**, 1700840.
- 114 M. Huo, Y. Zhang, M. Zeng, L. Liu, Y. Wei and J. Yuan, *Macromolecules*, 2017, **50**, 8192–8201.
- 115 S. Y. Khor, N. P. Truong, J. F. Quinn, M. R. Whittaker and T. P. Davis, *ACS Macro Lett.*, 2017, **6**, 1013–1019.
- 30 116 M. Huo, Z. Wan, M. Zeng, Y. Wei and J. Yuan, *Polym. Chem.*, 2018, **9**, 3944–3951.
- 117 M. Huo, M. Zeng, D. Wu, Y. Wei and J. Yuan, *Polym. Chem.*, 2018, **9**, 912–919.
- 35 118 B. Shi, H. Zhang, Y. Liu, J. Wang, P. Zhou, M. Cao and G. Wang, *Macromol. Rapid Commun.*, 2019, 1900547.
- 119 J.-M. Noy, A.-K. Friedrich, K. Batten, M. N. Bhebbe, N. Busatto, R. R. Batchelor, A. Kristanti, Y. Pei and P. J. Roth, *Macromolecules*, 2017, **50**, 7028–7040.
- 40 120 G. Delaittre and L. Barner, *Polym. Chem.*, 2018, **9**, 2679–2684.
- 121 J.-M. Noy, Y. Li, W. Smolan and P. J. Roth, *Macromolecules*, 2019, **52**, 3083–3091.
- 45 122 D. Le, D. Keller and G. Delaittre, *Macromol. Rapid Commun.*, 2019, **40**, 1800551.
- 123 Y. Pei, J.-M. Noy, P. J. Roth and A. B. Lowe, *Polym. Chem.*, 2015, **6**, 1928–1931.
- 50 124 Y. Pei, J.-M. Noy, P. J. Roth and A. B. Lowe, *J. Polym. Sci., Part A: Polym. Chem.*, 2015, **53**, 2326–2335.
- 125 N. Busatto, V. Stolojan, M. Shaw, J. L. Keddie and P. J. Roth, *Macromol. Rapid Commun.*, 2019, **40**, 1800346.
- 126 N. Busatto, J. L. Keddie and P. J. Roth, *Polym. Chem.*, 2019, **11**, 704–711.
- 55 127 S. Kubowicz, J.-F. Baussard, J.-F. Lutz, A. F. Thünemann, H. von Berlepsch and A. Laschewsky, *Angew. Chem., Int. Ed.*, 2005, **44**, 5262–5265.

- 1 128 H. Cui, Z. Chen, S. Zhong, K. L. Wooley and D. J. Pochan, *Science*, 2007, **317**, 647–650.
- 129 C. S. Gudipati, M. B. H. Tan, H. Hussain, Y. Liu, C. He and T. P. Davis, *Macromol. Rapid Commun.*, 2008, **29**, 1902–1907.
- 5 130 B. H. Tan, H. Hussain, Y. Liu, C. B. He and T. P. Davis, *Langmuir*, 2010, **26**, 2361–2368.
- 131 H. Hussain, B. H. Tan, K. Y. Mya, Y. Liu, C. B. He and T. P. Davis, *J. Polym. Sci., Part A: Polym. Chem.*, 2010, **48**, 152–163.
- 10 132 W. Du, Y. Li, A. M. Nyström, C. Cheng and K. L. Wooley, *J. Polym. Sci., Part A: Polym. Chem.*, 2010, **48**, 3487–3496.
- 133 C. Song, D. Ao, X. Wang, J. Zhang and Y. Tan, *Colloid Polym. Sci.*, 2013, **291**, 2815–2823.
- 15 134 F. Lv, Z. An and P. Wu, *Nat. Commun.*, 2019, **10**, 1–7.
- 135 F. Lv, Z. An and P. Wu, *Macromolecules*, 2020, **53**, 367–373.
- 136 Z. Li, E. Kesselman, Y. Talmon, M. A. Hillmyer and T. P. Lodge, *Science*, 2004, **306**, 98–101.
- 20 137 Z. Li, M. A. Hillmyer and T. P. Lodge, *Macromolecules*, 2004, **37**, 8933–8940.
- 138 Z. Li, M. A. Hillmyer and T. P. Lodge, *Langmuir*, 2006, **22**, 9409–9417.
- 25 139 A. N. Semenov, I. A. Nyrkova and A. R. Khokhlov, *Macromolecules*, 1995, **28**, 7491–7500.
- 140 Z. Li, M. A. Hillmyer and T. P. Lodge, *Nano Lett.*, 2006, **6**, 1245–1249.
- 141 C. Liu, M. A. Hillmyer and T. P. Lodge, *Langmuir*, 2008, **24**, 12001–12009.
- 30 142 Z. Li, M. A. Hillmyer and T. P. Lodge, *Macromolecules*, 2006, **39**, 765–771.
- 143 T. P. Lodge, A. Rasdal, Z. Li and M. A. Hillmyer, *J. Am. Chem. Soc.*, 2005, **127**, 17608–17609.
- 35 144 A. O. Moughton, T. Sagawa, L. Yin, T. P. Lodge and M. A. Hillmyer, *ACS Omega*, 2016, **1**, 1027–1033.
- 145 A. F. Thünemann, S. Kubowicz, H. von Berlepsch and H. Möhwald, *Langmuir*, 2006, **22**, 2506–2510.
- 40 146 Z. Li, M. A. Hillmyer and T. P. Lodge, *Langmuir*, 2006, **22**, 9409–9417.
- 147 R. R. Taribagil, M. A. Hillmyer and T. P. Lodge, *Macromolecules*, 2010, **43**, 5396–5404.
- 45 148 R. R. Taribagil, M. A. Hillmyer and T. P. Lodge, *Macromolecules*, 2009, **42**, 1796–1800.
- 149 Z. Zhang, X. Hao, P. A. Gurr, A. Blencowe, T. C. Hughes and G. G. Qiao, *Aust. J. Chem.*, 2012, **65**, 1186–1190.
- 50 150 G. Lopez, M. Guerre, J. Schmidt, Y. Talmon, V. Ladmiral, J.-P. Habas and B. Améduri, *Polym. Chem.*, 2015, **7**, 402–409.
- 151 W. F. Edmonds, M. A. Hillmyer and T. P. Lodge, *Macromolecules*, 2007, **40**, 4917–4923.
- 152 T. S. Kaminski, O. Scheler and P. Garstecki, *Lab Chip*, 2016, **16**, 2168–2187.
- 55 153 I. Platzman, J.-W. Janiesch and J. P. Spatz, *J. Am. Chem. Soc.*, 2013, **135**, 3339–3342.
- 154 T. Gao, X. Gu, S. Guo and G. Wang, *Polymer*, 2020, **205**, 122732.
- 155 D. A. Babb, B. R. Ezzell, K. S. Clement, W. F. Richey and A. P. Kennedy, *J. Polym. Sci., Part A: Polym. Chem.*, 1993, **31**, 3465–3477.
- 156 Y. Li, S. Zhang, L. Tong, Q. Li, W. Li, G. Lu, H. Liu and X. Huang, *J. Fluor. Chem.*, 2009, **130**, 354–360.
- 5 157 D. W. Smith, S. T. Iacono and S. S. Iyer, *Handbook of Fluoropolymer Science and Technology*, John Wiley&Sons, Inc., Hoboken, 2014.
- 158 L. Tong, Z. Shen, D. Yang, S. Chen, Y. Li, J. Hu, G. Lu and X. Huang, *Polymer*, 2009, **50**, 2341–2348.
- 10 159 D. Yang, L. Tong, Y. Li, J. Hu, S. Zhang and X. Huang, *Polymer*, 2010, **51**, 1752–1760.
- 160 Y. Li, S. Zhang, H. Liu, Q. Li, W. Li and X. Huang, *J. Polym. Sci., Part A: Polym. Chem.*, 2010, **48**, 5419–5429.
- 15 161 W. Yao, Y. Li, S. Zhang, H. Liu and X. Huang, *J. Polym. Sci., Part A: Polym. Chem.*, 2011, **49**, 4433–4440.
- 162 W. Yao, Y. Li, C. Feng, G. Lu and X. Huang, *Polym. Chem.*, 2014, **5**, 6334–6343.
- 20 163 W. Yao, Y. Li, C. Feng, G. Lu and X. Huang, *RSC Adv.*, 2014, **4**, 52105–52116.
- 164 C. Feng, C. Zhu, W. Yao, G. Lu, Y. Li, X. Lv, M. Jia and X. Huang, *Polym. Chem.*, 2015, **6**, 7881–7892.
- 165 G. Lu, H. Liu, H. Gao, C. Feng, Y. Li and X. Huang, *RSC Adv.*, 2015, **5**, 39668–39676.
- 25 166 H. Liu, S. Zhang, C. Feng, Y. Li, G. Lu and X. Huang, *Polym. Chem.*, 2015, **6**, 4309–4318.
- 167 R. Hoogenboom, *Angew. Chem., Int. Ed.*, 2009, **48**, 7978–7994.
- 30 168 C. Weber, R. Hoogenboom and U. S. Schubert, *Prog. Polym. Sci.*, 2012, **37**, 686–714.
- 169 F. Wiesbrock, R. Hoogenboom, M. A. M. Leenen, M. A. R. Meier and U. S. Schubert, *Macromolecules*, 2005, **38**, 5025–5034.
- 35 170 F. Wiesbrock, R. Hoogenboom and U. S. Schubert, *Macromol. Rapid Commun.*, 2004, **25**, 1739–1764.
- 171 T. Kagiya, S. Narisawa, T. Maeda and K. Fukui, *J. Polym. Sci., Part B: Polym. Lett.*, 1966, **4**, 441–445.
- 40 172 W. Seeliger, E. Aufderhaar, W. Diepers, R. Feinauer, R. Nehring, W. Thier and H. Hellmann, *Angew. Chem., Int. Ed. Engl.*, 1966, **5**, 875–888.
- 173 D. A. Tomalia and D. P. Sheetz, *J. Polym. Sci., Part A-1: Polym. Chem.*, 1966, **4**, 2253–2265.
- 45 174 T. G. Bassiri, A. Levy and M. Litt, *J. Polym. Sci., Part B: Polym. Lett.*, 1967, **5**, 871–879.
- 175 R. Ivanova, T. Komenda, T. B. Bonné, K. Lüdtké, K. Mortensen, P. K. Pranzas, R. Jordan and C. M. Papadakis, *Macromol. Chem. Phys.*, 2008, **209**, 2248–2258.
- 50 176 M. Lobert, R. Hoogenboom, C.-A. Fustin, J.-F. Gohy and U. S. Schubert, *J. Polym. Sci., Part A: Polym. Chem.*, 2008, **46**, 5859–5868.
- 177 K. Kempe, R. Hoogenboom, S. Hoepfener, C.-A. Fustin, J.-F. Gohy and U. S. Schubert, *Chem. Commun.*, 2010, **46**, 6455–6457.
- 55 178 U. Mansfeld, S. Hoepfener, K. Kempe, J.-M. Schumers, J.-F. Gohy and U. S. Schubert, *Soft Matter*, 2013, **9**, 5966–5974.

- 179 J. M. Bak, K.-B. Kim, J.-E. Lee, Y. Park, S. S. Yoon, H. M. Jeong and H. Lee, *Polym. Chem.*, 2013, **4**, 2219–2223.
- 180 J. M. Bak and H. Lee, *J. Polym. Sci., Part A: Polym. Chem.*, 2013, **51**, 1976–1982.
- 181 X. Jiang, F. Chun, G. Lu and H. Xiaoyu, *Polym. Chem.*, 2017, **8**, 1163–1176.
- 182 K. Matsumoto, M. Kubota, H. Matsuoka and H. Yamaoka, *Macromolecules*, 1999, **32**, 7122–7127.
- 183 K. Matsumoto, H. Mazaki, R. Nishimura, H. Matsuoka and H. Yamaoka, *Macromolecules*, 2000, **33**, 8295–8300.
- 184 K. Matsumoto, H. Mazaki and H. Matsuoka, *Macromolecules*, 2004, **37**, 2256–2267.
- 185 B. Fang, A. Walther, A. Wolf, Y. Xu, J. Yuan and A. H. E. Müller, *Angew. Chem., Int. Ed.*, 2009, **48**, 2877–2880.
- 186 X. Wang, K. Hong, D. Baskaran, M. Goswami, B. Sumpster and J. Mays, *Soft Matter*, 2011, **7**, 7960–7964.
- 187 S. Suárez-Suárez, G. A. Carriedo and A. Presa Soto, *Chem. – Eur. J.*, 2016, **22**, 4483–4491.
- 188 D. Presa-Soto, G. A. Carriedo, R. de la Campa and A. Presa Soto, *Angew. Chem., Int. Ed.*, 2016, **55**, 10102–10107.
- 189 D. R. Ratnaweera, U. M. Shrestha, N. Osti, C.-M. Kuo, S. Clarson, K. Littrell and D. Perahia, *Soft Matter*, 2012, **8**, 2176–2184.
- 190 Z. M. Hudson, J. Qian, C. E. Boott, M. A. Winnik and I. Manners, *ACS Macro Lett.*, 2015, **4**, 187–191.
- 191 B. Ni, M. Huang, Z. Chen, Y. Chen, C.-H. Hsu, Y. Li, D. Pochan, W.-B. Zhang, S. Z. D. Cheng and X.-H. Dong, *J. Am. Chem. Soc.*, 2015, **137**, 1392–1395.
- 192 J.-F. Gohy, N. Lefèvre, C. D’Haese, S. Hoepfener, U. S. Schubert, G. Kostov and B. Améduri, *Polym. Chem.*, 2011, **2**, 328–332.
- 193 P. Černoč, Z. Černočová, S. Petrova, D. Kaňková, J.-S. Kim, V. Vasu and A. D. Asandei, *RSC Adv.*, 2016, **6**, 55374–55381.
- 194 M. Guerre, J. Schmidt, Y. Talmon, B. Améduri and V. Ladmiral, *Polym. Chem.*, 2017, **8**, 1125–1128.
- 195 M. Guerre, M. Semsarilar, F. Godiard, B. Améduri and V. Ladmiral, *Polym. Chem.*, 2017, **8**, 1477–1487.
- 196 M. Guerre, M. Semsarilar, C. Totée, G. Silly, B. Améduri and V. Ladmiral, *Polym. Chem.*, 2017, **8**, 5203–5211.
- 197 E. Folgado, M. Guerre, A. D. Costa, A. Ferri, A. Addad, V. Ladmiral and M. Semsarilar, *Polym. Chem.*, 2020, **11**, 401–410.
- 198 E. Folgado, M. Mayor, V. Ladmiral and M. Semsarilar, *Molecules*, 2020, **25**, 4033.
- 199 E. Folgado, M. Mayor, D. Cot, M. Ramonda, F. Godiard, V. Ladmiral and M. Semsarilar, *Polym. Chem.*, DOI: 10.1039/D0PY01193B.
- 200 Y. Wu, L. Chen, X. Sun, J. Xu, G. Gu and J. Qian, *J. Saudi Chem. Soc.*, 2017, **21**, 713–719.
- 201 K. Vijayakrishna, D. Mecerreyes, Y. Gnanou and D. Taton, *Macromolecules*, 2009, **42**, 5167–5174.
- 202 J. Guo, Y. Zhou, L. Qiu, C. Yuan and F. Yan, *Polym. Chem.*, 2013, **4**, 4004–4009.
- 203 M. Isik, A. M. Fernandes, K. Vijayakrishna, M. Paulis and D. Mecerreyes, *Polym. Chem.*, 2016, **7**, 1668–1674.
- 204 H. He, K. Rahimi, M. Zhong, A. Mourran, D. R. Luebke, H. B. Nulwala, M. Möller and K. Matyjaszewski, *Nat. Commun.*, 2017, **8**, 14057.
- 205 A. H. Gröschel and A. Walther, *Angew. Chem., Int. Ed.*, 2017, **56**, 10992–10994.
- 206 V. Baddam, R. Missonen, S. Hietala and H. Tenhu, *Macromolecules*, 2019, **52**, 6514–6522.
- 207 H. Luo, Q. Tang, J. Zhong, Z. Lei, J. Zhou and Z. Tong, *Macromol. Chem. Phys.*, 2019, **220**, 1800508.
- 208 Y. Yang, J. Zheng, S. Man, X. Sun and Z. An, *Polym. Chem.*, 2018, **9**, 824–827.
- 209 D. Cordella, F. Ouhib, A. Aqil, T. Defize, C. Jérôme, A. Serghei, E. Drockenmuller, K. Aissou, D. Taton and C. Detrembleur, *ACS Macro Lett.*, 2017, **6**, 121–126.

Q23

15

20

25

30

35

40

45

50

55